

A state-of-the-art review on the utilization of machine learning in nanofluids, solar energy generation, and the prognosis of solar power

Santosh Kumar Singh, Arun Kumar Tiwari ^{*}, H.K. Paliwal

Department of Mechanical Engineering, Institute of Engineering & Technology, Dr. A.P.J. Abdul Kalam Technical University Uttar Pradesh, Lucknow 226021, India



ARTICLE INFO

Keywords:

Machine learning
Nanofluids
Solar energy
Perovskites
Forecasting technique

ABSTRACT

In the contemporary data-driven era, the fields of machine learning, deep learning, big data, statistics, and data science are essential for forecasting outcomes and getting insights from data. This paper looks at how machine learning approaches can be used to anticipate solar power generation, assess heat exchanger heat transfer efficiency, and predict the thermo-physical properties of nanofluids. The review specifically focuses on the potential use of machine learning in solar thermal applications, perovskites, and photovoltaic power forecasting. Predictions of nanofluid characteristics and device performance may be more accurately made with the development of machine learning algorithms. The use of machine learning in the creation of new perovskites and the assessment of their effectiveness and stability is also included in the review. Additionally, the paper explores developments in artificial intelligence, particularly deep learning, in this area and offers insights into techniques for forecasting solar power, including PV production, cloud motion, and weather classification.

1. Introduction

Machine Learning is a subset of Artificial Intelligence used to introduce a computer program. These programs are guided by a set of extensive data using some algorithms and statistics. Machine learning helps to track the data (by forecasting patterns or so). Machine learning constructs models for forecasting and develops heuristics to follow in later progress. Some of the Machine learning techniques uses a large set of data, makes specific patterns based on past data, and approximates the real future called Data Mining. It is to be noted that data mining is one approach to Machine Learning. Machine learning supports computers in modeling on the basis of experiences and thus forecasting future outcomes. Tom Mitchell gives the canonical definition of machine learning for the first time in 1997. In addition, he stated, “to learn from experiences concerning some class of tasks and performance measures”, he primarily focused on three things class of task, performance measures, and some well-defined experiences.

Machine Learning uses some approaches to perform this study (a) Supervised learning, (b) unsupervised learning [1,2], and (c) Reinforced learning. Classification is supervised learning, while clustering is relatively common in unsupervised learning [3,4]. Both supervised learning and clustering are studied in detail in the later section of the manuscript. Some of the widely used supervised techniques include (a) neural

networks, (b) support vector machines, and (c) decision trees [5]. Also, the majorly used clustering includes k-means [6]. The exercise of allocating an object to predefined categories is called Classification. Moreover, the process of segregating objects into groups/classes (in accordance with similarities) is known as Clustering. In the reinforced learning approach, a sequence of decisions is made where all these techniques have been discussed in the later section. Machine Learning techniques are widely used in modern manufacturing plants; the plants are equipped with a robust data acquisition system that collects and transfers data electronically from all the organization processes. Many variables are measured continuously, and their values are dignified at all phases continuously, these values are warehoused in the organization's databases. The measured records are correlated with product characteristics, raw materials used, environment (moisture, pressure, temperature, etc.), sensors, maintenance, production line, and other significant factors. Progress in research and development yields enormous data every day; this huge data availability draws attention to studying machine learning. Since the machine learning can predict the outcomes very close to the acceptable results, they are used to predict various properties (thermo-physical, transport, etc.) of nanofluids, phase change materials, drug delivery agents, etc. The adoption of machine learning is trendy in the arena of solar energy and is grooming in every aspect.

Deep Learning, ensemble learning, and linkage learning have been considered the most promising in machine learning. Machine Learning is

* Corresponding author.

E-mail address: aruntiwari@ietlucknow.ac.in (A.K. Tiwari).

Nomenclature			
<i>Abbreviations</i>			
1G	first generation	PA	product accuracy
2G	second generation	PAC	probably approximate correct
3G	third generation	PCE	power conversion efficiency
AC	ant colony	PSO	particle swarm optimization
AE	auto-encoder	PV	photovoltaic
AI	artificial intelligence	PVPF	photo-voltaic power forecasting
ANFIS	adaptive neuro-fuzzy interference system	RAP	rapid refresh
ANN	artificial neural network	RBF	radial base function
ANN-RBF	artificial neural network-radial basis function	RBFNN	radial basis function neural network
ARM	association rule mining	RCN	recursive convolutional network
BC	bayesian classification	RF	random forest
BOS	balance of system	RMSE	root mean square error
CART	category and regression tree	RNN	recursive neural network
CH	convex hull	RoBM	robust Boltzmann machine
CIGS	copper indium gallium di-selenide	SD	seasonal decomposition
CNN	convolutional neural network	SLFN	single layer feed forward networks
CNN-1D	convolutional neural network with 1D convolutional layer	SOM	self-organized map
CNN-2D	convolutional neural network with 2D convolutional layer	SVC	support vector classifier
CRBM	conditional restricted Boltzmann machine	SVM	support vector method
DBN	deep brief network	SVR	support vector regression
DC	direct current	UA	user's accuracy
DCNN	deep convolutional neural network	XRD	X-ray diffraction
DFT	density function theory		
DL	deep learning		
DNN	deep neural network		
DT	decision tree		
ELM	extreme learning machines		
FBNN	feedback neural network		
FFNN	feed-forward neural network		
GA	genetic algorithm		
GAN	generative adversarial network		
GAN—CNN	generative adversarial network convolutional neural network		
GB	gradient boosting		
GBR	gradient boosting regression		
GHI	global horizontal irradiance		
GMDH	group method of data handling		
GRNN	general regression neural network		
GRU	gated recurring unit		
HOIP	hybrid organic-inorganic perovskites		
ICA	imperialist competitive algorithm		
ICSD	inorganic crystal structure database		
IoT	internet of things		
KNN	k-nearest neighbour algorithm		
LR	logistic regression		
LS-SVM	least square support vector method		
LS-SVR	least square support vector regression		
LSTM	long short-term memory		
MAE	mean absolute error		
MAPE	mean absolute percentage error		
MIF	meteorological impact factors		
ML	machine learning		
MLPNN	multi-layer perception neural network		
MLR	multiple linear regression		
MP	the material project		
MPR	multilayer perception regression		
MR	multiple regression		
MSE:	mean squared error		
nMAPE	normalised mean absolute percentage error		
nRMSE	normalised root mean square error		
NWP	numerical weather prediction		
OA	overall accuracy		
<i>Symbols</i>			
e_k	looseness		
R^2	coefficient of determination		
S_k	activation factor		
θ_m	maximum distance between centers		
μ_{bf}	dynamic viscosity of base fluid		
μ_{nf}	dynamic viscosity of nanofluid		
σ^2	squared bandwidth		
B	bias value		
C	state of cell		
f	forget		
h	output of Long short-term memory		
H	output matrix of hidden layer		
J	fitting vector		
k	transfer function		
K	kernel function		
n	input value		
N_s	number of samples		
P	output predicted		
r_t	reset gate		
S_k	activation function of recurrent neural network		
t	time		
T	expected target		
U	weight matrix of gated recurring unit input to hidden		
V	connection weight		
W	weight matrix		
W'	weight matrix of gated recurring unit hidden to hidden		
X	input vector		
Z	Gaussian function		
Z_t	update gate		
θ	threshold		
μ	dynamic viscosity		
<i>Subscript</i>			
g	update		
hh	hidden layer		
hx	input layer		
i	input node		
j	hidden node		
o	output		
<i>Greek symbols</i>			
α	Lagrange multiplier		

Λ	number of centers	\emptyset	concentration of nanoparticle
β	output weight vector	ω	weight
Δ	weight vector	\odot	Hadmdard product
Φ	projector (one vector to another)	Γ	margin parameter

a subset of AI to introduce algorithms skilled enough of learning from a data set automatically. An artificial agent is needed to identify objects from their surroundings and foresee the behavior of their environment. During the preceding few decades, there is an unprecedented surge in generating and analyzing large data sets. The help of computers can efficiently perform computations that were not feasible a few eras ago. Dedicated computing tools like GPU- based machines are continuing this trend toward large-scale computation. Cheap, signifying that the “big data” revolution is increasing. The rapid increase in computability has been escorted by advanced learning techniques and analysis from huge data sets. The introduction of AI & ML in the mechanical fields is very much fascinating to researchers, and their application has quietly increased in the past few decades. Moreover, it becomes easy to predict the specific outcomes without actually doing the real-time experimentation as the technique utilizes past data sets to predict the outcomes; machine learning is nowadays used in almost all types of industry.

When pursuing machine learning, the study of AI related to IoT (Internet of Things) should be appreciated, as ML is a subset of AI. In previous decades IoTs are implemented in fault diagnostics and preventing cyber-crimes and monitoring the motor status [7,8]. Nowadays hybrid renewable energy system is also being used and their also ML techniques are gaining advantages, majorly used are wind-solar hybrid system [9]. It can also be remarked that machine learning impacts the practical cost of projects, for instance, when analyzing nanofluids with a trained model, the material cost is minimal compared to practical implementation cost, and inventory cost is reduced. It also reduces waiting time as results are obtained more quickly. However, this study only focuses on the subject matter of nanofluids and solar devices, and is discussed these matters in detail. For instance, Zhao et al. [10] used ANN data-driven modeling to predict nanofluid’s thermal conductivity and viscosity for automotive radiators. Ramezanizadeh et al. [11] used ML for dynamic viscosity modeling of nanofluids; ML techniques used were MLPNN, ANFIS, RBF, GMDH, and LS-SVM with ICA, and PSO. Bahraei et al. [12] used an ML algorithm to predict and optimize nanofluids; they included ANN, Fuzzy Logic, and hybrid AI methods.

The contribution of the authors and the novelty of the paper are discussed below:

- First, the study discusses the basic idea of machine learning implementation and techniques (algorithms) used in machine learning (Supervised learning/ Unsupervised learning and Reinforcement learning).
- Secondly, it reviewed the previous research done for evaluating the thermophysical properties of heat transfer fluids.
- Third, the readers gain the knowledge of potential applications of machine learning in solar devices (solar collectors and solar cells/ Perovskites)
- Fourth, the readers envisage the solar forecasting approaches by implementing machine learning techniques.
- Last, the review paper points out some promising research arenas of machine learning and recommendations for future studies.

This review covers the use of nanofluids for solar collectors, and solar cells for energy generation, with a focus on the application of machine learning techniques. The review explores the evaluation of thermo-physical properties of heat transfer fluids in solar collectors and the use of machine learning for optimizing the structure of perovskites in solar cells. The review also highlights the importance of solar forecasting in the study and implementation of solar devices. No comprehensive

paper covering all these aspects of solar energy generation has been published to date, according to the authors. The organizations of the manuscript in short are as; first introduction followed by machine learning implementation and techniques, then a short brief of Deep learning and then Constraints solving techniques. Then comes the application parts in which the authors discussed applications in nano-fluid, prediction of thermo-physical properties by ML. Then the authors discuss on power forecast factors (PVPF) and forecasting techniques by ML, and the conclusion and future works.

2. Machine learning implementation

Implementation of machine learning could be accomplished by following the set of processes. 1) Defining objectives of Research, 2) Constructing Dataset, 3) Mentioning descriptors cast off to designate the data, 4) Opting machine learning techniques according to purpose, 5) Constructing & optimizing machine learning models, and 6) Result evaluation and validation. The specifics of these tasks are found from various machine learning sources [13,14]; Fig. 1 shows the set of processes.

2.1. Objective setting

Implementing machine learning could serve various objectives; these objectives are to be clearly defined beforehand to perform pertinent stages and events, including selecting the best-suited ML technique. These machine learning practices are assembled and described in relation to the commission they can undertake. The commonly performed tasks that are performed by machine learning are *Description, Prediction, Clustering, Classification, and Association*. Generally, all these tasks have their usual meaning.

2.2. Constructing dataset

Datasets have been generated both in-house, i.e., from experimentation and computation, or mined from supplementary sources (publications or databases). This study demonstrates that readers can use different data sources. Data from experimental, computational, and research paper sources, for example, may be used to estimate nanofluid characteristics and evaluate heat transfer. Moreover, open-source datasets such as the Dortmund Data Bank are available for nanofluid research. Reliable data sources for the research of solar cells and perovskites include HOIPs, the Periodic table, DFT computed data, The Materials Project, and the JARVIS-DFT database.

2.3. Descriptors

Models in machine learning should be eloquent and convey useful connections amongst the input variables and certain response variables (outputs). The input data could be in any form continuous (e.g., Thermal temperature treatment) or categorical (e.g., perovskite-type), user-defined, measured, directly measurable etc. They are called as *features, factors, descriptors, or fingerprints*. They are used contingent on the devices, discipline, and viewpoint of the handler. Description choice plays a vital role in ML; they should clearly define the system to justify for the differences and similarities in response variables in anticipated accuracy and resolution. Researchers stated that description would be *reversible, eloquent, worldwide, and readily accessible* [15]. But the number of descriptors must be redundant and not associated. Ward et al. [16]

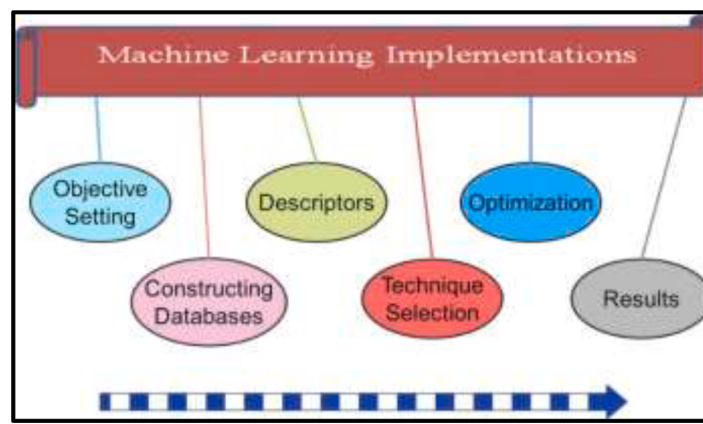


Fig. 1. Implementation techniques of ML.

reported possible descriptors that can be cast-off to predict material properties; they identified a total of 148 candidates; they too classify them into four classes basic property statistics, stoichiometric attributes, electronic property attributes, and ionic compounds. for design allied to atoms/ion, property and structure some commonly witnessed Descriptors were reported by Buttler et al. [17].

Not all the descriptors stated are used in all types of problems, descriptors that exclusively pronounce the data will be contingent on the objective or knowledge be wanted. The descriptors having less prominence in describing the system to avert overfitting (dataset containing a lesser amount of data points) must be eliminated. In such belongings, dimensionality reductions are required because simple models are informative and robust [13]; this is accomplished by eliminating feature choice descriptors (commissioning forward or backward eliminations). To lessen the dimensionality, build a reduced set of novel descriptors from the original list (feature mining) [13]. The other methods like machine learning techniques, optimization, and result validation will be done as usual; the learning methods are reviewed and discussed in the following sections.

2.4. Machine learning techniques

ML techniques are typically classified based on their task, which is further categorized within the machine learning paradigm studied in earlier sections. These tasks are categorized into three types: supervised learning, unsupervised learning, and reinforcement learning. The author has examined these categories in detail in Fig. 2; This study focuses The author's focus is on supervised and unsupervised learning, as these techniques are predominantly used (around 90–95%) in the mechanical field. Therefore, the study is limited to these two categories. The algorithm is demonstrated in Fig. 3.

2.4.1. Supervised learning

The supervised learning tends to learn, and output map, this type of machine learning algorithm has numerous input variables and a single output variable. Two separate tasks are performed by supervised learning: Classification and Regression. Classification predicts categorical output (discrete or nominal values, e.g., True, false, low, medium, high etc.); on the other hand, Regression is cast-off to envisage continuous or ordered value (e.g., price of a vehicle). Assessment of thermo-physical characteristics of the nanofluids and heat transfer prediction and efficiency ANN/ RBF/ GMDH/ ANFIS. The efficiency of the

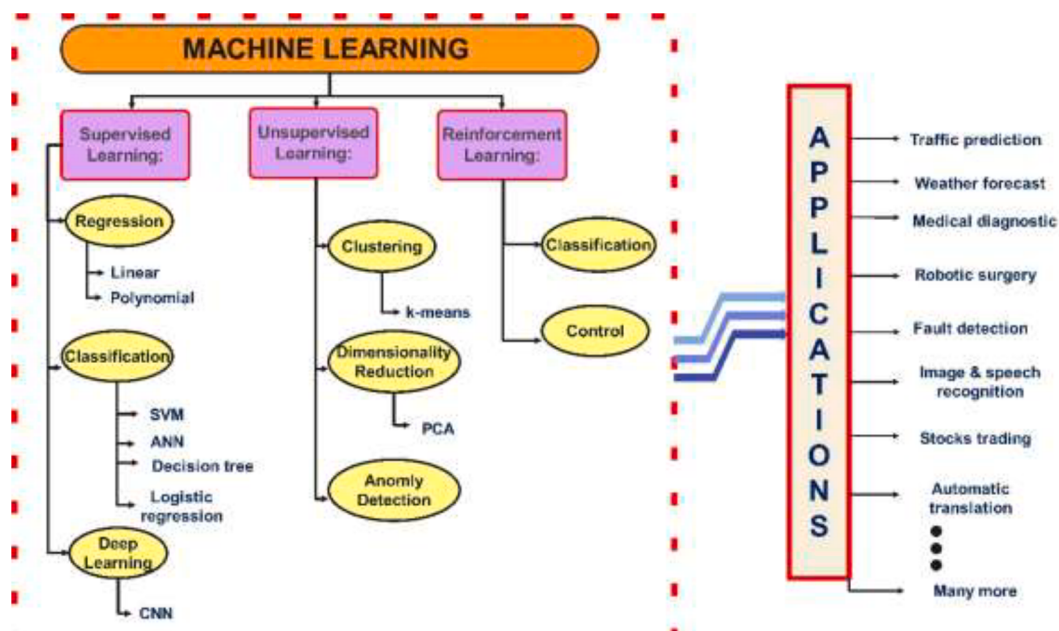


Fig. 2. Techniques and applications of machine learning [18].

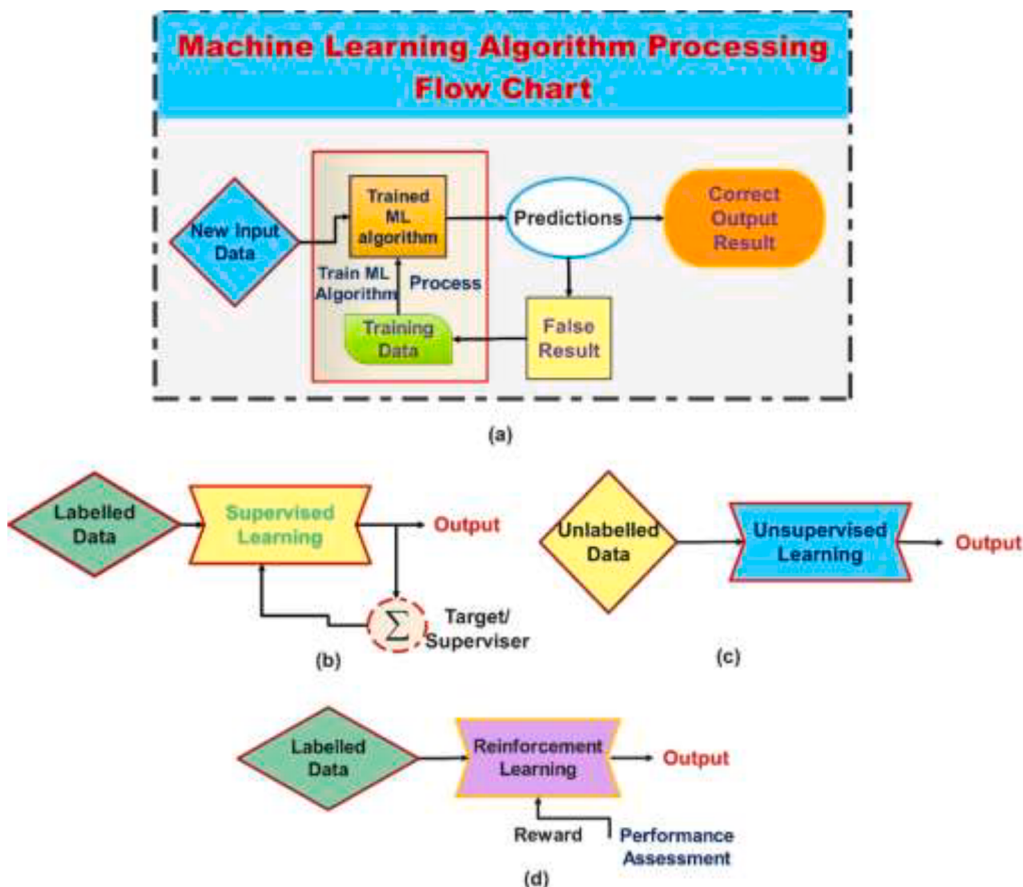


Fig. 3. Schematic showing ML processes [18].

perovskite cells can also be studied by the supervised learning approaches for instance GBR/ SVM/ RF etc. and other clustering techniques. All of them are discussed at the respective concerned sections.

2.4.2. Unsupervised learning

The unsupervised learning is cast-off to recognize symmetries and reliance on unlabeled data. This machine learning technique uses association rule mining, clustering, anomaly detection, density estimation, and representation learning. In unsupervised learning, the keen focus is on discovering patterns for the data points. In this study, unsupervised learning methods have been employed for solar prognosis applications, such as weather forecasting using GAN and LSTM, which will be discussed in the relevant sections. Although numerous machine learning techniques exist, the author will only focus on those that have been extensively studied and are crucial to the research. These techniques are as follows:

Classification: Classification comes under the study of supervised learning; this technique divides the data keen on classes encompassing a collection of output variables, they can be moreover categorical or could be categorized k-nearest neighbor (KNN) Algorithm, Decision Tree (DT), Logistic regression (LOR), Support Vector Method (SVM), Bayesian classification (BC), and Artificial Neural Network (ANN) are its machine learning techniques.

Clustering: Clustering is a type of unsupervised learning that the author is studying. This ML domain focuses on grouping data points based on the similarity of certain features. Clustering techniques are mainly of five types. (a) Partition clustering technique, (b) Hierarchical clustering methods, (c) Density-based clustering methods, (d) Grid-based methods, and (e) Model-based methods. Clustering is often used for dividing the huge dataset addicted to homogenous minor subsets to enhance effectiveness. k-means clustering is the modest form commonly

used, although hierarchical clustering is mostly cast-off in material investigation.

Description / Exploratory data analysis: It is a modest statistical investigation and explanation of data in graphical arrangements to look at its features and distinct subset manifestation [19]. Although the technique is quite cumbersome, some researchers use it reasonably appreciated on behalf of preliminary study, similar to meta-Analysis [20].

Estimation/ Prediction: These machine learning models the relation among independent input and dependent output variables to mark classical judgments. Procedures for instance Artificial Neural Network (ANN), Multiple Regression (MR), Random Forest (RF), Gradient Boosting Regression (GBR), and Support Vector Regression (SVR) are cast-off for this resolution. Despite ANN's being widely cast-off, ML practices can model non-linear relations effectively.

Association Rule Mining (ARM): ARM is used to ascertain the veiled connections amid the attributes (input and output) in huge databases besides tends to detect the variables (output variables) that appear in datasets. Apriori algorithm is the chief and modest cast-off for this resolution [14]; the subgroup discovery technique tends to introduce stimulating associations with dissimilar variables regarding the property of interest [21]; this method is used in material research also [22].

2.4.3. Some of ML techniques reviewed

The widely used ML technique embraces artificial neural network (ANN) for example Multi-layer perception NN (MLPN), Radial base function ANN (RBF-ANN), group method of data handling (GMDH), adaptive neuro fuzzy inference system (ANFIS) etc., Category and Regression Tree (CART), Random Forest (RF), Support vector method (SVM) (include least square support vector method) etc.

Multilayered perception neural network is the technique of merging the

biological system and intelligent computational approach. MLPNN is a typical approach cast-off in ANNs [23]. In this approach, there are three distinct layers consisting of various nodes. The first layer is the input layer, the second layer is the hidden layer, the intermediate layer, and the final layer is the output layer as demonstrated in Fig. 4. The forecasted result of ANN is given in the input layer; every node has a weight vector, which connects with other nodes in the successive layer. Every node of the MLPNN model has this structure for getting input, handling, and yielding output. Summation of all nodes in the input layer is done and move in as input for nodes of the hidden layer [24]. Let X is the input vector to MLPNN model, $X = [x_1, x_2, \dots, x_n]^T$ then:

$$n_j = \sum_{i=1}^n \omega_{ji} x_i + j, \quad j = 1, 2, 3, \dots, k \quad (1)$$

$$y_j = f(n_j) = f\left(\sum_{i=1}^n \omega_{ji} x_i + \theta_j\right) \quad j = 1, 2, 3, \dots, k \quad (2)$$

Where, n_j is input value of j^{th} node in the hidden layer. ω_{ji} is the weight amongst the connection j^{th} node and i^{th} input node. θ_j is the threshold of j^{th} hidden node, k is the transfer function that provides the complete input of hidden nodes in the hidden layer. Each function possesses its own unique properties. The output node is obtained by multiplying the output of each hidden node with its corresponding output linking weight, as described by the author. Since there is no established methodology for determining the appropriate number of hidden layer sizes, this factor should be carefully considered. The number of hidden layers can be adjusted according to factors such as problem complexity, noise level, and the amount of training and testing data available [25]. Neurons are often supplemented in the course of training to find optimal. Training stage establishment is essential for the MLPNN model.

Group Method of data handling (GMDH) first presented by Ivankhneko [27] in 1971 as a self-regulated neural network. It is a subset of inductive procedures for computer oriented mathematical modeling. A.G. Ivankhnenko invented the method superior to ANN due to its self-regulation feature; it also does not require any precondition definition like dynamic neurons, layers, or number of neurons. In this, repetitive practice is done to evaluate P's objective value to be satisfactorily precise in contrast to the real value. In GMDH modeling, modest quadratic equations are initially appreciated, but after some time, it becomes intricate [28]. For n input parameter and a single output, the Kolmogorov-Gabor, which is a high-order polynomial, is recognized by following equation:

$$P = \alpha_0 + \sum_{i=1}^n \omega_i X_i + \sum_{i=a}^n \sum_{j=1}^n \omega_{ij} X_i X_j + \sum_{i=1}^n \sum_{j=1}^n \sum_{k=1}^n \omega_{ijk} X_i X_j X_k + \dots \quad (3)$$

Where X is input vector ω is weight vector and P is output prediction by model. The least square method is cast-off to find the output of P by achieving the mean square error. For two input variables X_i and X_j the overall correlation of polynomial is given in Eq. (4):

$$P = \alpha_0 + \alpha_1 X_i + \alpha_2 X_j + \alpha_3 X_i X_j + \alpha_4 X_i^2 + \alpha_5 X_j^2 \quad (4)$$

A generalized schematic representation showing networks of GMDH is shown in Fig. 5.

Adaptive Neuro Fuzzy Inference System (ANFIS) method was firstly proposed by Jang [30] in 1993. In this method, there are five layers (actions are determined for each layer); the inputs are made fuzzy in the first layer based on fuzzy membership function (range 0–1) they are projected. In the second layer, the input signal is transformed, and the weight of the corresponding membership function is monitored. The third layer, referred to as the normalized layer, calculates the normalized firing strength of all nodes. In the fourth layer, defuzzification is carried out, and the final output is generated in the fifth layer, which consists of a single node that sums up all the input signals from the previous layers.

Radial Basis Function (RBF) network is a popular feed-forward neural network model known for its excellent estimation capabilities, straightforward structure, and fast training process. The network structure consists of three interconnected layers: an input layer, a hidden layer, and an output layer. Each layer is fully connected to the preceding one. The input layer receives the input values, which are then transmitted to the hidden layer. The hidden layer plays a crucial role in this network, using the radial basis function as its activation function, which computes the vector distance multiplied by an additional bias. The hidden layer's main function is to transform the input vector into a new space, and the data is then sent to the output layer through weighted connections [31]. The output from the hidden layer of j^{th} neuron is given by Eq. (5):

$$Z_j = Z\left(\|X - \Delta_j\|\right) = \exp\left(-\frac{\|X - \Delta_j\|^2}{2\xi_j^2}\right) \quad (5)$$

Where Z is RBF function (Gaussian function), X is the “input vector”, Δ_j is the “weight factor”, ξ_j is the “standard deviation”, standard deviation is given by Eq. (6) as:

$$= \frac{\theta_m}{\sqrt{\Lambda}} \quad (6)$$

where, θ_m is the “maximum distance between the centers”, Λ indicates the “number of centers”. Also, the hidden layer neurons weighted sum of signals received from the output layers:

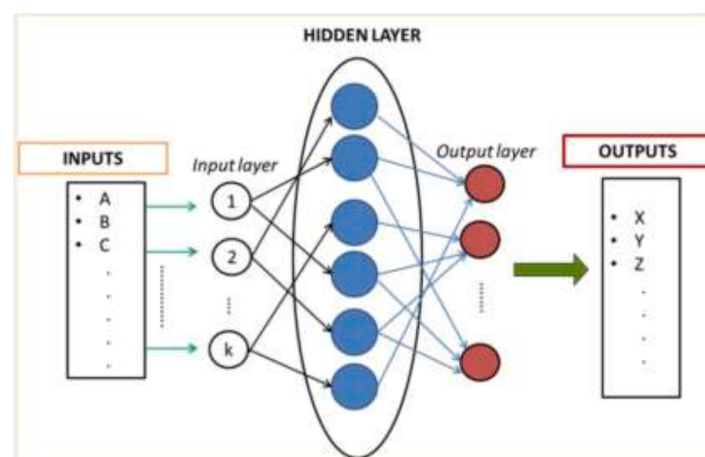


Fig. 4. ANN topology [26].

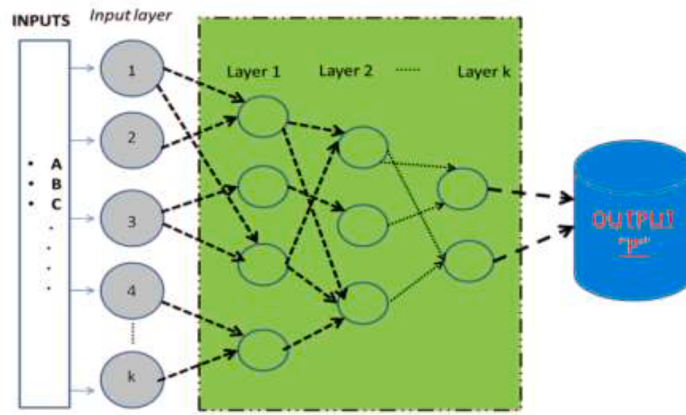


Fig. 5. Functionality of GMDH [29].

$$\gamma = \sum_{j=1}^k \omega_j Z_j \quad (7)$$

Where ω_j is the weight vector (computed in the training phase).

CART is an intuitive model; CART technique practices a decision tree and uses it as a prognostic method; it receives a cluster of training data as inputs to regulate which stuffs are most appropriate for segmentation.

Random Forest is a collection of numerous CART's. RF are the decision tree set having input variables running on multiple decision trees as shown in Fig. 6. Both CART as well as RF are easy to understand as they have a clear structure. But both have overfitting risks that limit their usage.

The support vector method (SVM) falls under the category of supervised learning models; SVM technique was familiarized and executed in 1999 by Suykens and Vandewalle. SVM can be cast-off for regression analysis, classification, and pattern recognition. The algorithm of SVM involves the placement of a classification hyperplane to optimize the boundary between positive and negative scenarios. This algorithm is advantageous for small sample sizes or high-dimensional data. However, it is essential to consider the kernel function as its performance primarily depends on it. Furthermore, SVM may present challenges when dealing with very large data sets, which could be considered a limitation of this approach. It cannot solve overfitting problems; therefore, LSSVM was established. In broad LSSVM nonlinear function is articulated as follows [23,33,34]. The characteristic of various ML algorithm are shown in Table 1

$$f(x) = w^T x + b \quad (8)$$

Where, "f" is the connection among inputs and target, "w" is the

Table 1
Characteristics of various ML algorithms.

Method	Application	Advantages	Limitations
ANN	Used for a large data set.	ANN can model complicated nonlinear relationships and generalization.	Requires high demand for computation due to large sample.
CART	When datasets are limited.	Easy structure.	Overfitting is easy.
RF	When the dataset is limited.	Can model multifaceted nonlinear relationship, stable, less risk of overfitting.	High noise data.
IANN	For large sample.	An intelligence algorithm optimizes network structures.	High demand for computation due to large sample size.
SVM	For small dataset.	Nonlinear regression and dimensional pattern recognition are particularly effective for small sample sizes.	Kernel function sensitiveness, difficulty in dealing with large samples.

weight vector, " \emptyset " projects x into the characteristic vector, and "b" is bias value [23,34–36]. A fitting error function is well-defined in the regression problem so that minimum topology involves [23,34–36].

$$\text{MinJ } (w, e) = \frac{1}{2} w^T w + \gamma \sum_{k=1}^m e_k^2 \quad (9)$$

The limitation equation is as follows:

$$y_k = w^T \emptyset(x_k) + b + e_k \quad (10)$$

$$k = 1, 2, 3, \dots, m$$

γ is the margin parameter, e_k is looseness of x_k [23,34–36].

Lagrange multiplier of α_i can be used to obtain unlimited form of LSSVM technique. Here limitation equation is not required [23,34–36].

$$L(w, b, e, \alpha) = J(w, e) - \sum_{k=1}^m \alpha_k \{w^T \emptyset(x_k) + b + e_k - Y_k\} \quad (11)$$

The prime mode of the problem is described by Karush-Kuhn-Tucker (KKT) by considering various state parameters of w , b , e , and α and is given by Eq.(12) [23,34–36].

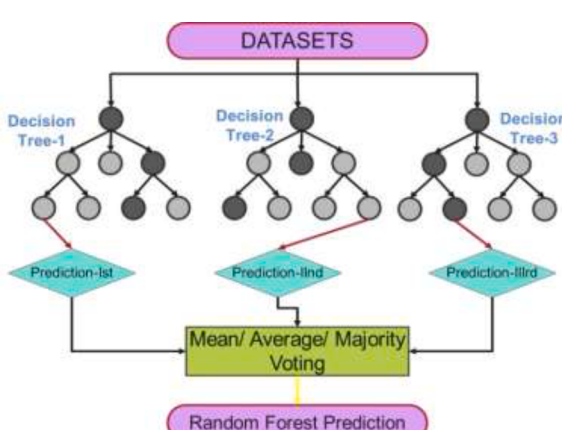


Fig. 6. Showing random forest tree [32].

$$\left\{ \begin{array}{l} w = \sum_{k=1}^m \alpha_k \phi(x_i) \\ \sum_{k=1}^m \alpha_k = 0 \\ \alpha_i = \gamma e_i \\ w^T \phi(x_i) + b + e_i - Y_i = 0 \end{array} \right\} \quad (12)$$

And the linear expression is given by Eq.(13) [23,34–36].

$$\begin{bmatrix} 0 & -Y^T \\ Y & ZZ^T + \frac{1}{\gamma} \end{bmatrix} \begin{bmatrix} b \\ \alpha \end{bmatrix} = \begin{bmatrix} 0 \\ 1 \end{bmatrix} \quad (13)$$

Where variables Y, Z, and α are $\{Y = Y_1, \dots, Y_m\}$, $Z = \phi(x_i)^T Y_i, \dots, \phi(x_m)^T Y_m$ and $\alpha = [\alpha_1, \dots, \alpha_m]$ respectively. Kernel function of $K(X, X_k) = \phi(X)^T \phi(X_k)$, $i = 1, 2, \dots, m$, the LSSVM regression is evaluated as follows [23,34–36].

$$f(x) = \sum_{k=1}^m \alpha_k K(x, x_k) + b \quad (14)$$

Kernel expressed as [23,34–36].

$$K(x, x_k) = \exp(-\|x_k - x\|^2 / \sigma^2) \quad (15)$$

Where the σ^2 is squared bandwidth. The squared bandwidth is a significant factor on behalf of any optimization method like a genetic algorithm (GA). The objective function of the LSSVM optimization algorithm is the mean squared error. MSE can be evaluated as:

$$MSE = \frac{\sum_{i=1}^n (predicted\ value - actual\ value)^2}{ns}$$

In which ‘ns’ is the number of samples as of the original population.

Coefficient of determination (R^2) is the alternative indicator that is cast-off to validate the delicacy of the model by indicating a linear relationship among appraised and real output from experiments and evaluated as follows:

$$R^2 = 1 - \frac{\sum_{i=1}^n (measured_i - estimated_i)^2}{\sum_{i=1}^n (measured_i - average(measured))^2}$$

3. Deep learning

Deep Learning (DL) or Deep Neural Network (DNN) is a state of ML technology. It is also a type of ANN that uses sufficient hidden layers, advanced learning algorithms, ambient input data, and useful analyzing parameters [37]. DL and DNN fall in the category of unsupervised ML techniques, which means the DL algorithm can envisage the outcomes by analyzing the input pattern. Hinton first anticipated DL in 2006 as “layer-wise greedy learning” [38]. DNN is a subset of machine learning; it is a model of networks consisting of neurons and containing numerous layers and parameters amongst input and output. It executes the neural network architecture technique, thus called a deep neural network.

Its representation is hierarchically at several layers and provides automatic learning features. This advanced feature makes it a robust learning approach. Thus, in short, DL architecture is used for alteration processes and feature extraction. The DL model is best suited for dealing with more extensive data and complex problems [39]. Due to its vast applicability and usage, DL is frequently called a Universal Learning Method. The method of DL is exceptionally scalable in terms of computation and data. ResNet-21 is a deep network developed by Microsoft and was implemented as a supercomputing scale. In this study, the major portion is based on the machine learning approaches but this topic is intended to gain an overview of deep learning approaches to the readers. DL is capable of predicting local optima and depicting assembly rates with ease. The author’s study focuses on the following deep learning mechanisms in particular, which are highly recommended for solar applications. The section delves into these models in detail: (a)

Recurrent Neural Network (RNN), (b) Long Short Term Memory (LSTM), (c) Gated Recurrent Unit, (d) Restricted Boltzmann Machine (RBM), (e) Deep Brief Network (DBN), (e) Autoencoder (AE), and (f) Deep Convolutional Neural Network (DCNN) [40,41].

3.1. Recurrent neural network (RNN)

When it comes to sequential or time-series data ‘RNN’ which is a class of artificial neural networks is mainly used. The characteristic of time series data is it comprises temporal intrinsic data that cannot be executed by conventional neural networks [42]. RNN possesses an supplementary time step edge which presents a key of time to the neural network [43]. A cycle of self-connection of neurons is formed by the edges called recurrent edges by connecting the adjacent stages [44]. The self-connected loops in a neural network represent the passage of time steps. Each hidden unit is connected to a hidden state vector (h_t) that is initialized to zero at the start. The hidden state vector has the same length as the number of units and retains important information from past iterations. The feedback connection allows the hidden state at time t to retrieve the hidden state vector from the previous time instance (t-1). The previous hidden state vector, along with the current input (x_t), is used to compute the hidden state vector for the current time instance (t). As a result, the network’s output is influenced by both the current input and the previously stored information in the hidden state vector. The Eqs.(16) and (17) presents the mathematical processing:

$$h_t = f(W_{hx}x_t + W_{hh}h_{t-1} + B_h) \quad (16)$$

$$\hat{y}_t = f(W_{yh}h_t + B_y) \quad (17)$$

Where $f(\cdot)$ shows the activation function, W_{hx} and W_{hh} shows the weight matrix amongst the input and hidden layer and hidden layer with itself at preceding time steps, correspondingly. The bias vectors are represented by B_y and B_h . The readers will find an algorithm-based study of RNN in the forecasting of solar powers in the later section also, this topic finds understanding of basic RNN deep learning mechanism.

3.2. Long short-term memory (LSTM)

Long Short-Term Memory (LSTM) is a successful implementation for time series prediction problems, which is an addition and an improved type of RNNs. Researchers studied the incapacitated behavior of RNN networks in supervision of long-term dependences in data, and the cause may be due to vanishing gradient and gradient explosion problems [45]. The issue is being addressed by the execution of LSTM network familiarized by Sepp Hochreiter and Jürgen Schmidhuber [46]. LSTM architecture addresses the vanishing gradient issue by using the memory cells and gates, which govern the flow of information in the network. LSTM network encompasses the following gates: input gate i_t , forget gate f_t , update gate (g_t) and output gate (o_t) as shown in Fig. 7. These mathematical expressions illustrate the operation, where the forget gate plays a critical role in the architecture by controlling the amount of information that should be eliminated from the memory cell. The weight matrices of forgetting, input, update, and output gate are signified by w , w_i , w_g and w_o respectively while the biases of the forget, input, update, and output gate are represented by b_f , b_i , b_g , and b_o . Sigmoid function is applied in forget gate on the output of the last state (h_{t-1}) and input data (x_t) and given by Eq. (18):

$$f_t = \sigma(w_f[h_{t-1}, x_t] + b_f) \quad (18)$$

Sigmoid function σ is used by the input gate to determine which value to write, and the update gate adopts $tanh$ activation function to make new cell values.

$$i_t = \sigma(w_i[h_{t-1}, x_t] + b_i) \quad (19)$$

$$g_t = \tanh(w_g[h_{t-1}, x_t] + b_g) \quad (20)$$

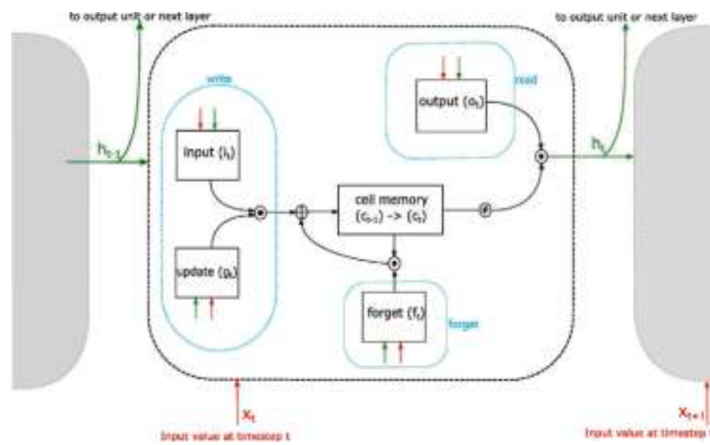


Fig. 7. Structure of LSTM [40]. Figure Reprinted with permission from Elsevier LN 5,482,480,120,201.

The state of the previous state (C_{t-1}) interrelates with the update gate to update the new state of the cell (C_t).

$$C_t = f_t * C_{t-1} + i_t * g_t \quad (21)$$

At last, the output gate governs the output of the cell, this gate is joined with a cell state which is activated with \tanh activation function to get the output (h_t):

$$o_t = \sigma(w_o \cdot [h_{t-1}, x_t] + b_o) \quad (22)$$

$$h_t = o_t \tanh(C_t) \quad (23)$$

3.3. Gated recurring unit (GRU)

One of the standard variants of RNN is the Gated recurring unit, first familiarized by Cho et al. [46] in 2014. The primary goal of the algorithm is to address the vanishing gradient problem in RNNs and enable them to capture long-term dependencies in data. Due to their similar working mechanisms and designs, the performance of GRUs can be compared to that of LSTMs. Like LSTMs, GRUs also incorporate a gating mechanism to regulate information flow. However, GRUs utilize a single update gate that comprises both an input gate and a forget gate. GRU has two gates: update gate (z_t) and a reset gate (r_t). These gates elect the vital information to be reserved and irrelevant to be removed from the past

data as shown in Fig. 8. The mathematical expression is discussed below in Eq. (24). First, the update gate is cast to choose the information needed and computed at time ‘t’ as follows:

$$z_t = \sigma(w_z x_t + u_z h_{t-1}) \quad (24)$$

Where σ is sigmoid activation function, x_t is input to the model, w_z and u_z are the weight matrices and h_{t-1} conveys information from the previous time step (t-1). Also, the reset gate dictates the past information be forgotten as:

$$h' = \tanh(Wx_t + r_t \odot Uh_{t-1}) \quad (25)$$

Where W and U show the weight matrix amongst the input to hidden and hidden to hidden layer correspondingly. The Hadamard product is evaluated amongst (r_t) and Uh_{t-1} . The current state hidden value is evaluated by the update gate as follows:

$$h_t = z_t \odot h_{t-1} + (1 - z_t) \odot h' \quad (26)$$

3.4. Restricted Boltzmann machine (RBM)

The Restricted Boltzmann Machine uses input data to predict the probability distribution; it is stochastic. The most used application of RBM is collaboration, collection of data, dimension reduction, and filtering [47]. Recent advancements or hybridization of RBM have been done these are; Conditional Restricted Boltzmann Machines (CRBMs) [48], Discriminative Restricted Boltzmann Machine (DRBMs) [49], and Robust Boltzmann Machine (RoBM) [50].

3.5. Deep brief network (DBN)

Hinton did further modifications leading to the weighted architecture of RBM, which is known as Deep Brief Network. In essence, the Deep Belief Network combines the properties of Restricted Boltzmann Machines (RBMs) with those of a classifier, allowing it to train hidden data with similar attributes to RBMs. This type of arrangement ensures that, upon completing the first iteration, the output of the first layer serves as input for the subsequent RBM layer, as depicted in Fig. 9. This operation is continued till it extends the output layer [51]. Hence, progressively it can learn patterns after completing the learning process; the distinctive patterns of the data set can be recognized. 3D objects can be identified by the pattern recognition ability of the Deep Brief Network [52]. It is still in the developing phase, and the research is going on image recognition and speech recognition hybrid models [53–55].

3.6. Autoencoders

Autoencoders (AE) is another approach to deep learning. AEs can

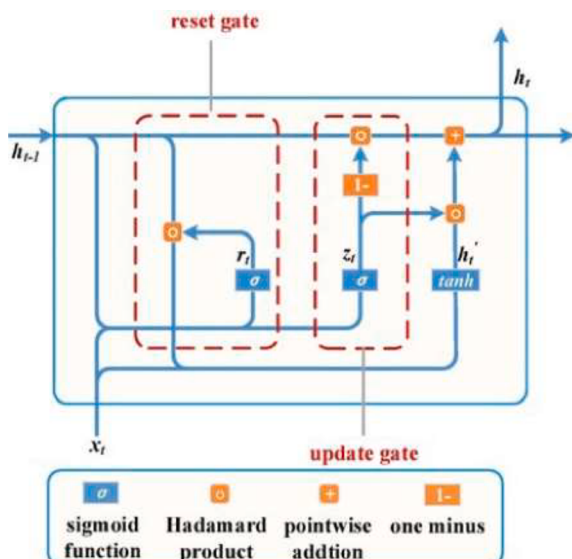


Fig. 8. Structure of GRU [40] Figure Reprinted with permission from Elsevier LN 5,482,480,120,201.

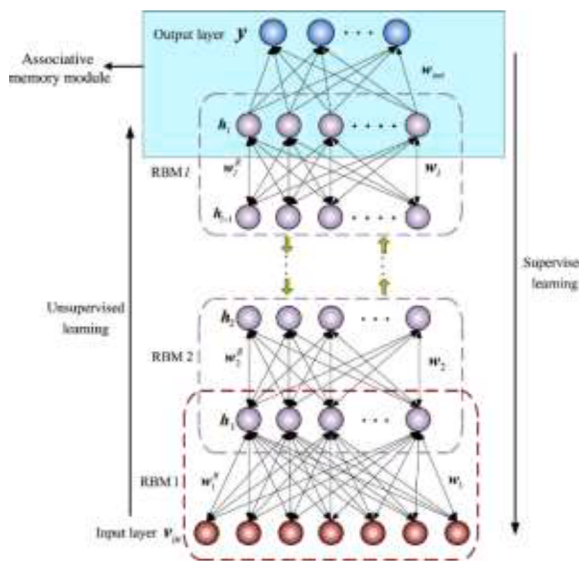


Fig. 9. Structure of DBNN [40] Figure Reprinted with permission from Elsevier LN 5,482,480,120,201.

study different models of data to predict forecasting [56]. However, it falls in the regime of the unsupervised learning approach. The information is encoded from the input layer and decoded later after reconstruction. Noise can be successfully filtered out during data extraction, this being the main advantage of AEs.

3.7. Convolutional neural network (CNN)

Convolutional Neural Network (CNN) is a particular subset of the DL algorithm. It is used to diagnose patterns by merely emphasizing the edges and pixel behavior recognized in numerous images in its layers. CNN nowadays is the finest tool for face recognition, speech recognition, image classification, behavior recognition, and machine handwriting recognition. Noncognition [57] is the computational model utilized in CNN; it depends on linear or non-linear filters to extract image topographies. CNN has several blocks like activation, convolutional, and pooling. All work was collected for extraction and transformation [58]. CNN comprises four layers [59]; (a) Convolutional layer, (b) Pooling layer, (c) fully connected layer, and (d) Logistic regression layer. In the diagram, Fig. 10. In order to extract features from the input data, the convolutional layer is utilized, and these features are combined by the pooling layer, which reduces the resolution of the feature maps and aggregates the input features. Following the pooling layer, there is a fully connected layer, and then the logistic regression layer. The fully

connected layer transfers the learned distributed feature to a unified space to facilitate high-level reasoning, with all neurons in the current layer being linked to those in the preceding layers.

CNN bears many advantages over traditional fully connected neural networks; one of them is CNN, which has reduced the number of parameters to be evaluated and the reason being the weight sharing mechanism. Also, CNN consists of small Kernel sizes; this effectively extracts hidden structures and inherent features. Some other structural performance benefits of CNN are CNN has practical functionalities, like outstanding data processing with grid topology mechanism [61]. The application of CNN is commonly seen in image processing techniques. In applications of PVPF, weather classification is not commonly used [62]. Hybrid CNNs are invented for further enhancement of performances. Recursive Convolutional Network (RCNs) [63] is a type of hybrid CNN. Convolutional Restricted Boltzmann machines are developed by incorporating RBMs in CNN [64]. Hu et al. [65] studied de-noising AE and integrated it with DL with a to foresee wind power production for new wind farms. Qureshi et al. [66] studied the utilization of ML for short-term wind power forecasts. Some researchers [67] studied SOM and LVQ can distinguish previous PV output data. Chen et al. [68] in their research, the authors explored the use of self-organized maps (SOM) to identify local weather patterns for next-day forecasts from online time-series data. While SVM and KNN methods are suitable for smaller sample sizes, they may not be effective for larger quantities of complex data due to their shallow learning models. To address this issue, the authors propose the use of a CNN, which can capture deep non-linear relationships between input and output variables.

Gao et al. [69] studied a deep generative model by using the LSTM approach for multi-step solar irradiation prediction. Data and temperature forecasts were cast-off for training and testing, their results show an effective reduction in error accumulation. The model produces a 7.7% accuracy improvement against the traditional LSTM regression model. Wang et al. [70] studied day-ahead PV power forecasting to accomplish advanced PV power output and lessen the influence of random fluctuations. Traditional artificial intelligence (AI) modeling techniques may face issues with overfitting and lack of adequate generalization capabilities, especially when it comes to complex nonlinear modeling. Aiming to overcome the challenges posed by conventional artificial intelligence (AI) modeling techniques, this study proposes a deep learning model with time correlation implemented under the partial daily pattern prediction (PDPP) framework. The study involves using an LSTM-RNN model for independent day-ahead PV power forecasting, with adjustments made based on time correlation. Additionally, a PDPP method is proposed to enhance the accuracy of the output pattern. The detailed analysis of solar PV power forecasting by different artificial intelligence technique is suggested in the later sections of the manuscript.

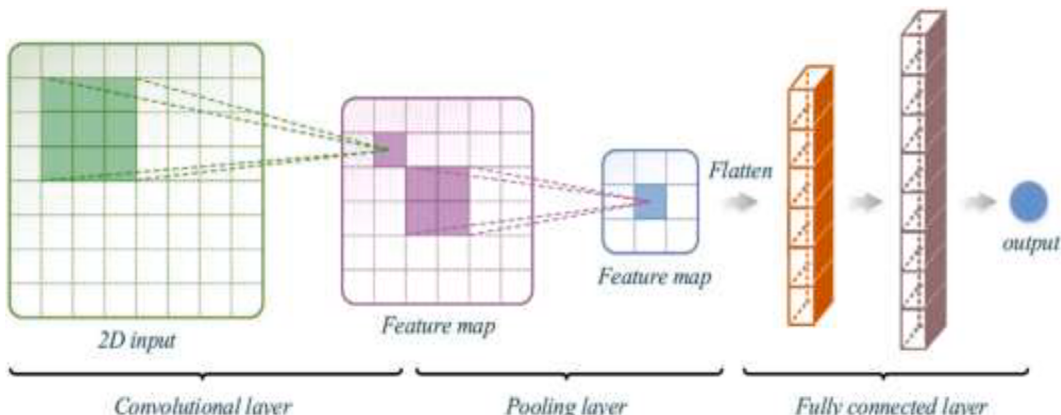


Fig. 10. Showing structure of CNN [60] Figure Reprinted with permission from Elsevier LN 5,482,480,496,735.

4. Constraints solving in machine learning techniques

Constraints can be handled in a variety of settings and applications, such as complicated product and service setups, manufacturing schedule determination, online sales suggestions, and optimization challenges. Optimization issues were solved in this work to optimize non-dimensional correlations between the Richardson number, Nusselt number, and Reynolds number with pressure decrease [71]. Constraints are implemented to ensure sufficient runtime performance and enhance prediction quality. This review introduces constraints solving paradigms, for instance, constraints satisfaction [72], SAT solving [73], and answer set programming [74] with some key concepts of machine learning.

4.1. Constraints satisfaction problems (CSPs)

Constraints on variable sets express limits on possible combinations of assignments of variables [75], CSPs stipulate problems in relation of possible value combinations [75]. Preferably, the assignments must embody each variable and satisfy every constraint introducing the problem, some of the examples are covered in the literature [76]. Backtracking search united with forward checking (analyzes the extent of impact variables on other assigned variables) is one of the basic approaches to solve CSP and different methods promise consistency properties for instance node consistency and arc consistency. Readers are appreciated to refer for a general overview of CSP in the article [75]. Evaluation criteria cast-off for predicting the conduct of Solver are (a) Runtime (time required to find the solutions), (b) Optimality (optimization of solutions concerning optimization function), (c) Accuracy (correctness of classifications), and, (d) Completeness (amount to which present solutions found). The supervised machine learning technique is the leading ML method for solving constraints as compared to the unsupervised and reinforcement learning approaches. Carbonell et al. [77], discussed the primary classification of machine learning methods. The below section is discussing constraint satisfaction. Constraint learning supports constraint learning which often aids to evade the redundant search and improves the performance of the search. Machine learning is employed to predict solutions for constraint-specific problems (CSPs). Additionally, satisfiability prediction involves forecasting the satisfiability of a CSP without using a solver. Heuristic learning focuses on developing search heuristics, which ultimately improve the prediction quality and runtime performance of the constraint solver. Constraint learning uses the derivation of constraints from datasets based on feedback from user experts for knowledge acquisition.

The moto of this study is to recognize formerly unfamiliar constraints of CSP and speeds the process of search. Gent et al. [78] studied a model based on the classification that aids to recognize CSP illustrations on which the learning is predicted to enhance the performance of the solver. Also, the study reveals that one cannot expect improvement in the performance by the constraint learning always. A decision tree-based approach is introduced by Gent et al. [78] that aids to appraise a given CSP. The researcher adopted lazy learning in the context of nogood learning, nogood can be understood as attribute value grouping, which fails to permit the determination of solution. This type of nogoods can be expected as extra constraints which must take into account for solver. Some of the examples cast-off in the decision tree approach of the author are number of variables, attributes, problem constraints, constraint that refers to specific variables.

Wang and Tsang [79] propose a neural network architecture that aids to figure out CSP. A CSP variables and potential values are encoded as nodes of the neural network. With the study authors concluded that the solution of CSP based on neural network is feasible, the author presents car scheduling example in his study. A neural network learns pertinent assignments on basis of training data which is denoted by previously executed CSPs. Adorf and Johnson et al. [80] studied multi-neural network architecture for executing binary CSPs, in which

the concern of local minima is processed by the merging of so-called auxiliary guard networks. Continuous exploration is used to permanently progress the solver's search behavior [81]. The approaches have two primary modes (a) Functioning mode (used to execute concrete user problem), (b) Exploration mode (continuously improves the search performance for training the heuristic model). Arbelaez et al. [79] investigated the idea of permanent lifetime learning which to continuously become an application domain expert. Galassi et al. [82] studied a related neural network approach to exercise heuristics. Continuous improvement of the search performance is the key to reinforcement learning which establishes the clue of successively discovering new problem-solving techniques with the ultimate goal of cultivating the problem-solving behavior and outputs [83,84,85,86]. Spieker et al. [87] familiarize reinforcement learning techniques for successfully executing constraint satisfaction problems. The reinforcement learning technique did not depend on datasets cast for evaluation and emphases further on the instance by instance training.

Combinatorial optimization is associated with the activity of evaluating an optimal solution for given constrained problem [88,89]. Guerri and Milano et al. [90] used decision tree learning for Bid Evaluation Problem (BEP) which is considered as a combinatorial optimization problem. They introduce the uses of decision tree to adopt the solving approaches for testified evaluation scenarios which are integer programming (IP) and constrained programming (CP). Bonfietti et al. [91] introduce a method to integrate Decision tree (DTs) and Random Forest (RFs) in a constrained programming model. The main cause for the merger is domain constraints and heuristic parts of the model. The impression is to acquire extra constraints that are then added in the model. This type of technique can be considered as the empirical model learning where past solution data are used to infer mentioned models. In many contexts, optimization and runtime prediction are crucial. Within the framework of solution space learning, runtime estimation can help evaluate the suitability of a particular knowledge base in interactive settings. The goal is to support solver runtime prediction. A regression-based study is done by Hutter et al. [92] where problem instances are cast as primary indicators for runtime prediction.

4.2. Constraint learning

Raedt et al. [93] introduce knowledge acquisition scenarios that can be merged as inductive learning processes for figuring out constraints that support test/ training data. the task varies from learning processes with the scope of solver session in which the trained constraints are chiefly cast to enhance the solver performances [78]. Learning constraints from datasets is a crucial task that addresses challenges in knowledge acquisition bottleneck, especially in industries that rely on constraint-based models. Collaborative constraint training is also possible within the context of active learning processes.

4.3. SAT solving

There are two primary methods for integrating ML in the cause of solving problems, [94]. First ML can be cast directly to execute individual SAT instances as in the case of given input SAT problem, the algorithms learn to solve the problem instance itself [82]. Another one is heuristic methods cast machine learning for the sake of executing necessary heuristics which are then solved by solvers to get the results [94]. Apart from the search solution, there are other uses of ML efforts in SAT solving which comprises the characteristics of picking the good algorithm and predicting satisfiability for solving a known problem instance.

A tactic to introduce neural networks for categorizing SAT problems in terms of satisfiability is studied by Selsam et al. [95]. In this, problems are encoded as the graph in which all nodes depict one literal problem as shown in Fig. 11. Adding on each clause reveals a node of neural work which is jointed to literals that are part of the clause. Furthermore, a

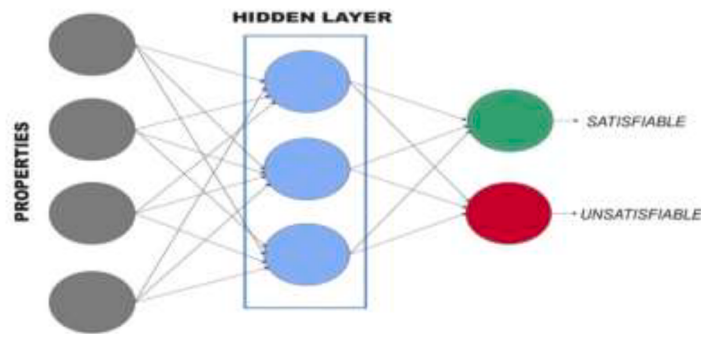


Fig. 11. SAT programming structure [87].

neural network used to foresee the satisfiability of SAT and determine a solution.

4.4. Answer set programming (ASP)

Gebser et al. [96] introduce a method for solver selection regarding ASP scenarios. The study of the author reveals how to select solver configuration, and the features of problem used by the ML approaches for instance support vector regression, these features further cast to record a known problem to a hopeful solver configuration. In 2020 Yang et al. [97] proposed a roadmap called NeurASP to integrate neural networks into answer set programs. The approach involves utilizing the neural network output to grade atomic facts in ASP. This integration is considered an effective example of merging symbolic AI (ASP) and sub-symbolic AI (neural networks). The Fig. 12. shows the working of ASP.

Since the paper is a review paper the authors had addressed the machine learning works in the studied domain of solar energy, as far as the Parameters of the Machine Learning are concerned the section navigates the readers to a basic understanding of the concepts. Model performance is mainly determined by varieties of parameters. Every algorithm of machine learning has two types of model parameters: (a) Ordinary parameters, (b) hyper-parameters. Ordinary parameters are automatically optimized/learned in the training phase of the model. While hyper-parameters typically set by the programmer/ user manually before the training of the machine learning model. Also, one should appreciate that hyperparameters are used to derive the ordinary parameters. And the hyperparameters are derived from the heuristics.

The hyperparameters are the standard parameters that work in every condition/ circumstance. They are known as a necessary component of the model. One does not have to adhere to the default settings (only if the calls for it, one can perform changes). Datasets like training, testing, and validation are vital as they can adjust the parameters to achieve the

required accuracy and evade breaching of data. The coefficients and the weights of the algorithm extracted from the data are referred to as the model parameters. In the case of ANN, the weights represent the model parameters. Conversely, in the case of Support Vector method, the support vectors serve as the model parameters, while in regression (logistics and linear regressions), the coefficients represent the model parameters. The model parameters in neural network models consider the influence of predictor variables on the target variable. While during the learning phase hyper-parameters are dependent on the behavior of the algorithm. It is vital to appreciate that each algorithm consists a different set of hyperparameters, for instance, the depth parameter for the decision tree. The following points show the metrics that measure the administration of the model

- Confusion Matrix: it is the table that defines how classification is executed on datasets smoothly.
- Accuracy: it is the score that is produced when the class is generalized. The ability of the model to generalize suitably.
- Recall: it governs the model's ability to predict the true data points as true data points.
- Precision: It designates the quantity of data points the model recognizes and how many are genuinely positive.

5. Applications of ML in nanofluids

Nanofluids are the innovative generation of reinforced imperial fluids, widely used in all class research and development, and received considerable attention in recent decades. Nanomaterials are nano-engineered entities [98–100]. The working domain of nano-engineered fluid is vast, and they are widely used in Solar collectors [101–103]; Although metallic nanoparticles are used in various fields, the author's study focuses solely on their use in solar collectors. The addition of these small metallic nanoparticles to a base fluid results

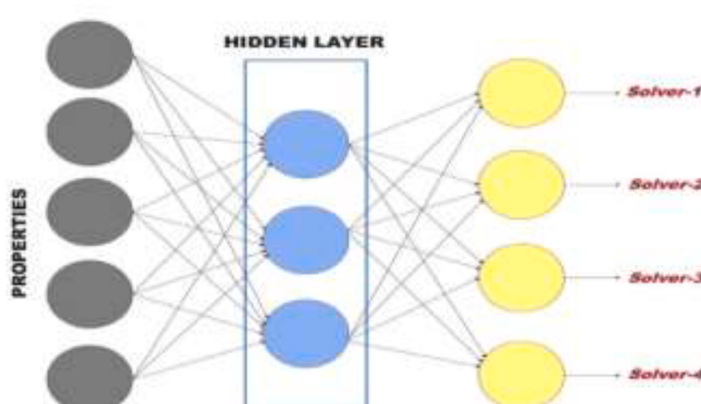


Fig. 12. Structure of ASP [87].

in fluids with improved thermo-physical properties and enhanced heat transfer. The appellation nanofluid was coined in 1995; various studies have been directed to study the amalgamation, synthesis, thermo-physical properties, thermo-fluid characteristics, and nanofluid application. From 2008 to 2018, in around 10 years, the research papers publications increased by 327.8% [104], and in 2019 over 4300 research papers are submitted in the web of science databases. These nano-engineered fluids have very complicated thermo-physical properties since their effect on heat transfer, fluid flow, and optical and radiative performance is nonlinear; here arrives the machine learning domain, although challenging to perform but can give the required results with an acceptable range. This topic covers in time review of the ML investigation and progress of heat transfer with nanofluids; machine learning on behalf of predicting thermo-physical characteristics of nanofluid, thermal hydrodynamic enactment of heat exchangers, optical and radiative performance of nanofluid in the solar energy system.

6. ML of thermo-physical properties

Predicting the thermo-physical properties of nanofluids accurately is a complex task due to various factors that influence these properties, such as the concentration, size, shape, and type of nanoparticle, pH, shear rate, suspension temperature, and the method used to prepare the base fluid [11], flow condition etc. For instance, many researchers reported fabrication using different nanoparticles such as CNTs [105], Al_2O_3 [106], Ag [107], Cu [108], CuO [109], graphene [110], SiC [111], MgO [112], TiO_2 [113], and Ni [114] due to above all reasons, the determination of thermo-physical property of nanofluid is tough.

ANN has been extensively functional to numerous arenas because the learning mechanism (internal) is very standardized; for this reason, the ANN technique is used to envisage nanofluid thermo-physical stuffs. The method requires both the input variable and the output variable. Input variables could be nanoparticle type, base fluid type, temperature, pressure, the concentration of particles, volume fraction etc. similarly, output variables can be thermal conductivity, dynamic viscosity, and specific heat. The output variable mentioned can be calculated using an internal learning algorithm. It is important to note that a large sample size is required for performing ANN. Additionally, it is possible to combine ANN with intelligent algorithms such as PSO, SA, and AC to form an Intelligence Algorithm-based ANN (IANN). The size of the sampling data is also very significant in the ML methods [115–118]. In cooperation, small and large data size affects the workability of the data set. Too small data set causes a random or systematic error which gives a highly undetermined mode fit. While large data sets will sustain high overheads in data fabrication, compilation, and storage. Thus, choosing the optimum data size for this approximate correct (PAC) learning may be used to easily test learnability for a specific quantity of samples [119, 120]. PAC learning checks if the sample size is adequate over empirical risk minimization by ensuring the realization assumption of the ML algorithm.

ANN algorithm through a 3 input model and 4 input model respectively is cast-off by Longo et al. [121], and the thermal conductivity is predicted of oxide water nanofluid; the researcher decided that the best fit R^2 of testing model of 3 input is not satisfactory. Toghraie et al. [122] foresee the viscosity of nanofluid (Ag/ethylene glycol (EG)) using ANN model; input variables taken are temperature and volume fraction of nanofluid. Many researchers have used ANN algorithms to model unlike systems with utmost accurateness [123–126]. Toghyani et al. [127] executed the ANN algorithm to model solar Stirling engines and perceived that the net-work and torque of Stirling engines might be anticipated accurately by using the ANN model. Loni et al. [128] model a parabolic dish collector for its thermal performance by using ANN and concluded by comparing between output model also genuine data attained from the experimental study; the ANN algorithm precisely foresees the thermal performance the R^2 was 0.99. Ahmadi et al. [129] used the GMDH-ANN algorithm for modeling the thermal conductivity

of alumina/water and alumina/EG nanofluid. They investigated that input variable are temperature and concentration in the first condition, and nanoparticle size was input data for second condition. The result shows that via size of particle in comparison to concentration and temperature (case-1) leads to further precise model. Thus, in view of all-important variables in ML methods is indispensable to attain accurate model.

In conventional nanofluids, nanostructures are of a single type having nanoparticles and nanotubes cast-off as a solid phase in a liquid as base fluid [130,131]. These classes of nanofluids are apparent to compose and worthwhile in very operations. The metallic particles dispersed in the liquid undergo a perceptible influence on heat transfer properties as the metallic particles also have high thermal conductivity, also the dynamic viscosity increases by adding these nanosize particles. Still, the increment in dynamic viscosity is subjected to various other parameters such as concentration, temperature etc. the correlation technique is applicable for evaluating the dynamic viscosity very easily. Esfe et al. [130] investigated a correlation technique to estimate the dynamic viscosity of "ZnO-EG" nanofluid. The parameters were size= 18 nm, range of temperature= 24.7 °C- 50 °C and volume concentration= 0.25% - 5%. Temperature and concentration were used as the input variables, formulation obtained for dynamic viscosity is given by Eq. (27):

$$\frac{\mu_{nf}}{\mu_b} = 0.9118 \exp(5.49\phi - 0.00001359T^2) + 0.0303 \ln(T) \quad (27)$$

ANN model is also used to envisage the dynamic viscosity [132]; the ANN model's accuracy compared to correlation is also high as ANN has a very complex structure [133]. Esfe et al. [134] cast-off ANN algorithm and calculate the dynamic viscosity of TiO_2 /water as a function of temperature and mass function. He made a simple ANN algorithm with one hidden layer and four neurons. The solution obtained was very precise with R^2 value = 0.9998.

Group Method of Data Handling as discussed in Section 2.4.3 is an appropriate type of ANN model [129]. The GMDH method can be used when there is limited availability of data, and it is considered to be a powerful approach [135]. Shahsavar et al. [136] used GMDH to compute both thermal conductivity and dynamic viscosity; temperature, concentration, and shear rate are the input variables. R^2 and RMSE values obtained were 0.96 and 0.0018.

Baratpour et al. [137] correlate with calculating the dynamic viscosity of SWCNT/EG nanofluid, concentration of the nanofluid concentration ranges from 0.0125 to 0.1%, and the temperature varied from 30 to 60 °C. Esfe et al. [138] conducted a study on the impact of nanoparticle size on the thermal conductivity and dynamic viscosity of "Fe/water" nanofluid. Nanoparticles with diameters of 37, 71, and 98 nm were used, and the study found that increasing the size of the nanoparticles resulted in a higher dynamic viscosity ratio (nanofluid to base fluid) and thermal conductivity. Esfe et al. [139] modeled the dynamic viscosity of Fe-EG nanofluid by ANN, considered the size and concentration of particles and temperature and obtained high model accuracy with a maximum error of 2.5%. The computation cost of a model is linked to its size, which is determined by the structure and type of artificial neural network (ANN) used, including the number of layers, neurons, and the training function employed. While a complex structure model can deliver highly accurate results, it comes with higher computational costs.

Some models can be investigated to execute the thermo-physical characteristics of more than one nanofluid type [140]. Atashrouz et al. [141] smeared one of ANN models (GMDH) for nine distinct nanofluids. Basefluids were EG, propylene glycol, water concentration, nanoparticles' diameter, and temperature being the input variables, and the output was relative viscosity (nanofluid to base fluid). Their model was very precise, and the regression coefficient was 0.9978. Another researcher Aminian [142] studied an ANN model for eight water-based nanofluids with different types of nanoparticles such as metal oxides and

carbonic; he also used size, the concentration of nanoparticle, and temperature as input models; the obtained results are $R^2=6.66\%$ and $AAD=0.9842$.

Also, as far as the hybrid nanofluids are concerned, they contain multiple materials as nano-structure [23,143]. Most commonly used are carbonic nanostructures (e.g., MWCNTs and SWCNTs) [144]; they have weak modified properties as compared to conventional nanofluids [145]. But their synthesis is a cumbersome activity as compared to the conventional one. Their modeling approach is similar to that of conventional (input variables are mostly the same). But in the case of hybrid nanofluids correlation found via curve fitting, it is easy to evaluate the dynamic viscosity [146]. Asadi et al. [147] studied curve fitting technique to appraise the dynamic viscosity of MgO-MWCNT/EG nanofluid concentration range = 0.1–1% and temperature range = 30–60 °C; the proposed correlation was given by Eq. (28) the figure Fig. 13, shows the maximum error between the correlation and experimental results:

$$\frac{\mu_{nf}}{\mu_b} = [0.191\phi + 0.240(T^{-0.342}\phi^{-0.473})]\exp(1.45T^{0.120}\phi^{0.58}) \quad (28)$$

Maddah et al. [148] studied the dynamic viscosity of MWCNT–carbon/SAE 10 W40-SAE 85 W 90 was anticipated by using concentration and temperature as the input variables. The algorithm was excellent for predicting the dynamic viscosity with $R^2=1$. Some of the property characterization of nanofluids by ML are shown in Table 2.

6.1. ML in nanofluid heat transfer and heat exchanger

Heat exchangers are essential devices used in energy systems; they are primarily used to augment energy efficiency and improve thermal performance. In previous ages, nanofluids have been studied in various types of heat exchangers for instance plate heat exchangers (PHE), double pipe heat exchangers, and shell and tube heat exchangers. It is a piece of the necessary equipment in the renewable and sustainable energy industry. Wang et al. [157] and Xie et al. [158,159] used the ANN algorithm to study the heat transfer and friction factor for shell and tube heat exchangers. Zdaniuk et al. [160] proposed that the ANN model was sound appropriate for helically finned tubes. Symbolic regression-based correlations are compared with ANN [161].

Yet, the hydrodynamic and thermal study of the heat exchanger with nanofluid is very cumbersome. ML would be a boon in these incomprehensible cases, though it is not studied in detail. In this reading, the input variables include dimension and concentration of nanoparticles, thermal conductivity, viscosity, Reynolds number, Prandtl number, etc., and the Nusselt number, heat transfer coefficient, Pressure drop, etc. are the output variables. Wijaysekara et al. [162] studied the ANN

algorithm for the performance forecast of the compact heat exchanger by EBaLM-OTR methods. Maddah et al. [163] studied the ANN model to evaluate the energetic efficiency without using experimental data or extensive numerical data. The error between ANN predictions and experimental data was within an acceptable range. For the optimization process, the ANN model was used. Nusselt number and Heat transfer coefficient results were also enhanced, pressure drop is abridged as related to the base fluid. Minimum pressure drop and maximum heat transfer were achieved via the ANN model; the Genetic Algorithm was also utilized to study the heat exchangers with nanofluid. Nasirzadehroshenin et al. [164] studied the trained networks with GA; in this study, the target function of exergy efficiency is deliberated when the ANN model is used in the optimization process to make the best use of the fitness value with the least MSE error. A robust correlation between experimental data and the prediction of ANN-GA is obtained. A study performed using multi-objective optimization of Al₂O₃-water nanofluid in flat tube by via computational fluid dynamics, ANN, and genetic Algorithm techniques. To establish broad applicability of machine learning, it is of supreme importance to inaugurate enormous databases applicability of machine learning, it is of supreme importance to inaugurate enormous databases used for training and learning. Table 3 shows studies reported in utilization of ML in heat exchangers.

6.2. Application of machine learning in solar devices

Nowadays, ML seems to be an interdisciplinary aspect and is used in a variety of fields for faster and economic prediction of program-specific outcomes; researchers are focusing more on this eco-friendly source of energy. The integration of tools or concepts of machine learning boosts the workability of this regime. Machine learning generally circumvents problematical physical and mathematical models [169,170]; on a broad scale, they are used for modeling and optimizing solar collectors having nanofluid as working fluid [71,170–175]; machine learning techniques for instance ANN and GA are the utmost acceptable means. Risi et al. [171] proposed an optimization method for a new solar transparent parabolic trough collector that uses gas nanofluid to achieve maximum heat transfer efficiency of 62.5% and a volume fraction of 0.3, as well as an outlet temperature of 650 °C. The optimization method used was the Genetic Algorithm (GA). In a study by W. Ajbar et al. [176] multivariate inverse artificial neural network is used to provide a new technique of enhancing the efficiency of parabolic trough collector input parameters for the study were rim angle, inlet temperature of the fluid, ambient temperature, flow rate wind speed, and solar irradiance. Their result revealed that ANN achieved satisfactory results having coefficient of determination of 0.9511 and rMSE of 0.0193. The figure shows the

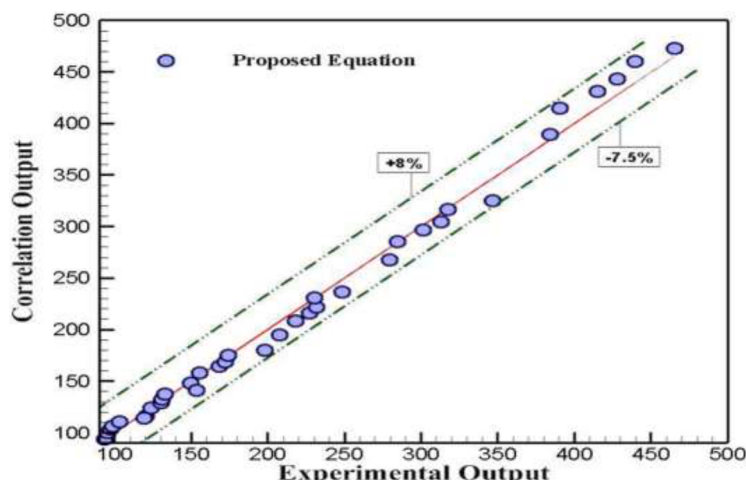


Fig. 13. Variation of correlation results with the experimental results [147] Figure Reprinted with permission from Elsevier LN 5,547,021,298,686.

Table 2

Property characterization of nanofluids by machine learning techniques.

Nanofluid	ML technique	Description	MAPE	R ²	Refs.
Oxide-water	ANN	Input data- thermal conductivity of nanoparticle, temperature, size of the cluster, and concentration. Output data- thermal conductivity.	0.6310	0.9910	Longo et al. [121]
Fe/EG	ANN; correlation	Input data- temperature and volume fraction. Output data- dynamic viscosity.	–	–	Toghraei et al. [122]
Al ₂ O ₃ /water	LS-SVR; SOM; BP	Input data- volume concentration, temperature and size of particles. Output data- thermal conductivity.	–	0.88125;0.88393;0.8999	Ahmadi et al. [129]
Al ₂ O ₃ -MWCNT/5W50	ANN; correlation	Input data- shear rate, volume fraction and temperature. Output data- viscosity	0.07;7.30	0.998;0.982	Esfe et al. [149]
Paraffin-Fe ₃ O ₄	GMDH	Input data- mass fraction, concentration, and temperature. Input data- thermal conductivity and dynamic viscosity.	–	0.96	Shahsavar et al. [136]
MWCNT-TiO ₂ , water-EG molten salt	ANN; correlation	Input data- volume fraction, temperature. Output data- thermal conductivity.	1.845;2.415		Akhgar et al. [150]
Al ₂ O ₃ -water	ANN	Input data- change in temperature, pressure, diameter, and percent weight. Output data- viscosity.	–	0.992	Hasanpour et al. [151]
TiO ₂ , Al ₂ O ₃ , CuO in carboxymethyl cellulose water	ANN	Input data- temperature and concentration. Output data-thermal conductivity.	1.60	–	Hojjat et al. [152]
Molten salt	ANN	Input data- mass fraction, temperature and size. Output data- specific heat.	–	0.9992	Hassan et al. [153]
ZnO/water	ANN; RBF; ANFIS	Input data- fluid inlet temperature, incident radiation, ambient temperature. Output data- efficiency and fluid outlet temperature.	0.7777;0.7481;0.8110/ 0.6330;0.5054;0.4882	0.9897;0.9923;0.9934/ 0.9363;0.9906;0.9896	Kalani et al. [154]
CNT/water	ANN; ANFIS; LS-SVM	Input data- Prandtl number, volumetric concentration. Output data- Nusselt number.	–	0.981;0.972;1	Baghban et al. [155]
Diamond-COOH, MWCNT-COOH in water	ANFIS; ANN	Input data- temperature, density, viscosity, volume. Output data thermal conductivity and kinematic viscosity.	0.02744;0.162940;0.01636;0.0842/ 0.09998;0.00047;0.00096;0.0007/ 0.09894;0.09275;0.02877;0.04617	–	Alrashed et al. [156]

Table 3

Machine learning techniques in heat exchangers.

Nanofluid	ML technique	Description	MAPE	R ²	Refs.
SiO ₂ -water	ANN	Input data- geometric progression, Prandtl number, Reynolds number, concentration. Output data- energetic efficiency.	0.92		Maddah et al. [163]
CNT/CuO water	ANN/GA	Input data- concentration, Reynolds number, cavity diameter ratio. Output data- exergy efficiency.	0.92		Nasira zadehrashenin et al. [165]
Al ₂ O ₃ -water	CFD/ANN/GA	Input data- flat-tube internal height, wall shear stress, volumetric flow, heat flux. Output data- heat transfer coefficient.	0.19;0.1967	0.9741;0.9719	Safikhani et al. [166]
Cu-carboxymethyl cellulose water	ANN/GA	Input data- diameter, concentration, radius ratio. Output data- change in pressure, heat transfer coefficient.	0.999;0.999		Bahiraei et al. [167]
TiO ₂ -Al ₂ O ₃ water	ANN/LINMAP/ TOPSIS	Input data- concentration, thermal conductivity, Prandtl number, Reynolds number. Output data- Nusselt number, change in pressure.	0.9952;0.9992		Hojjat et al. [168]

graph of thermal efficiency experimental and simulated obtained by established ANN model.

Sadeghi et al. [175] studied the exergy in the additional energy efficiency of evacuated tube solar collector by via Cu_2O -water nanofluid. The researcher compared the outputs of multi-layer perceptron (MLP) and radial basis function (RBF) models of ANN and stated that MLP model is further precise than RBF. All the technique (ANN, fuzzy logic, PSO, GA, SA and hybrid technique) have been used for the design of solar energy system [177,178], but only a limited study involves the usage of nanofluid [178,179]. In one study by Esmaeili et al. [180] the effect of hybrid nanofluid and turbulators is studied on the efficiency augmentation of the parabolic trough collector system, in their study the heat transfer coefficient, entropy, viscous entropy, Bejan number and friction coefficient is studied. The study reveals that employing turbulators and adding hybrid nanofluid improves the performance of the parabolic trough collector. In this study domain, the author restricts the study to PV cells and Perovskite cells with the integration of Machine Learning and the forecasting of PVPF.

6.3. Application of machine learning in the domain of PV cell

Photovoltaic (PV) is considered “the safest and cleanest technology” among other renewable energy sources. PV cells are discovered in the 19th century from then; there are many advancements in the PV domain in terms of their efficiency, solar cell type, and technology [181,182]. The technological PV system is primarily a power system that consists of an arrangement of well-interconnected components that work with one another and lead to electricity formation by sunlight energy. The system utilizes the generated energy, inverts it and stores it. PV system (centralized utility-scale or distributed) entails two regimes: (a) Solar cell and (b) Balance of System technology (BOS). Generation of electrical energy out of solar irradiation is done by cells, whereas the balance of the system (BOS) is crucial for chemically shielding, connecting, and mounting cells into panels.

Solar cells are the building blocks and are the key components of PV system. It is a device that right away transforms light energy (energy of photons) to direct current (DC) electricity, and the process of conversion is known as the Photovoltaic effect. The photons with high dynamism usually cross the bandgap of the material causing electric current and voltage. The broad classifications of solar cells are (a) first generation (1 G), (b) second generation (2 G), plus third-generation (3 G). Crystalline silicon water-based cells are 1st generation, 2 G encompasses crystalline silicon water-based as Cadmium Telluride ($CdTe$), Amorphous silicon (a-Si), Copper Indium Gallium di-Selenide (CIGS), and Single-Junction Gallium Arsenide (GaAs) cells. In contrast, the third-generation (3 G) comprises the latest advancements in the technology of organic materials and multi-junction cells. Kalani et al. [154] studied a hybrid ANN in addition PSO method to know the connection of input/ output

constraints and optimize a PV/T nanofluid-based collector structure at a system level. Table 4 shows Some of the studies of machine learning applications in solar field.

6.4. Machine learning in the domain of perovskites

The concept of ML has been extensively cast-off for numerous purposes, such as the discovery of new perovskites. Perovskite Solar Cell work initiates by replacing the dye with Methylammonium Lead Iodine $MAPbI_3$ in dye-sensitized solar cells [187], the specialized power conversion efficiency (PCE) has augmented to 25.2%. Initially, the prime concern was to increase the efficiency, and then stability comes into consideration, but stability remains a key challenge in Perovskite technology. Today the most important research area is developing new perovskite-like materials with high stability and acceptable bandgap. This study reports perovskite works established on computational data and works on experimental dataMost of these studies focus on ML analysis of computationally generated data, often using Density Functional Theory (DFT). The research based on computational data includes; Kim et al. [188] reported the optimum structures, dielectric constant, band gaps, and relative energies using DFT calculation and the outcomes are validated by theoretical/experimental data, the data source is 1346 HOIPs (DFT), and the involved ML technique is clustering. In 2017 Schmidt et al. [189] studied to estimate thermodynamic stability for screening and reported that a convex hull is used to determine stability, 2000 specimens were used to train the ML algorithm, and the remaining testing purpose techniques used were ANN, RF, and DT.

Alam et al. [190] used the ANN technique to study bandgap and Ruddlesden-Popper phases., he obtained data sources from 220 perovskites from periodic tables and performed DFT simulations and ML, and selection for octahedral factor and radioactivity was studied. Lu et al. [191] studied bandgap by screening the data source in [188,189] and 5158 from the periodic table; he used ML to foresee band gaps of 5158 HOIPs and used KRR, SVM, DT, GBR, and MPR (GBR was best). Takashi et al. [192] also studied band gaps by using the Random Forest Technique. RF is used to evaluate perovskite's bandgap using 18 descriptors and reported 10 firm perovskites with a proper bandgap. Xu et al. [193] used data sources from 590 single and 538 double perovskite s from The Materials Project & ICSD. They studied formability. Based on characteristics corresponding an atomic number, ionic radii, tolerance, electronegativity, and octahedrality factors, the formability analysis is done, and monitored by ML model for 367 $A_2B'B''O_6$ compounds.

Chaudhari et al. [194] studied screening for choosing suitable inorganic material; the ML techniques used are DT, GB, KNN, MLP. The data are screened by spectroscopy. 5097 materials data are taken from JARVIS-DFT database. Im et al. [195] take data from the periodic table (DFT generated 540 double halide perovskites) to envisage heat generation and bandgap; the ML technique used was GBRT eliminated

Table 4
Implementation of machine learning in the nanofluid based solar energy system.

Nanofluid	ML technique	Description	Application	R ²	Refs.
Al_2O_3 -EG/ water	ANN	Input data- particle diameter, temperature, and Reynolds number. Output data- volume fraction (optimum).	Solar collector	0.9992	Ebrahimi Moghadam et al. [183],
Silver/ water	ANN	Input data- heat flux, inlet temperature, and flow rate. Output data- Heat transfer coefficient, efficiency, outlet temperature.	Solar collector		Tomy et al. [174]
Grapheme oxide/ water	ANN	Input data- depth and length of collector, flow rate, concentration. Output data- collector efficiency and Nusselt number.	Solar collector	0.99828;0.99814	Delfani et al. [184]
ZnO-water	ANN	Input data- atmospheric temperature, inlet temperature, incident radiation. Output data- electrical efficiency, outlet temperature.	PV/T system	0.9934;0.9906	Kalani et al. [154]
SiC-paraffin wax	ANN	Input data- ambient temperature and solar irradiance.	PV/T system	0.842;0.652;0.633;0.972	Al-Waeli et al. [185]
SiC-water/ paraffin wax	MLP/SOFM/ SVM	Input data- solar irradiance, cell temperature. Output data- current, electrical efficiency.	PV/T system	0.74308;0.94753;099,662	Al-Waeli et al. [186]

correlated topographies and statistical analysis and cast-off to predict features. GBRT was used to examine heat generation and band gaps. Jain et al. [196] studied bandgap, stability, and structure by screening the data set taken from [197,198] MP, and used SVM for the analysis. SVM and the convex hull were used to measure bandgap and structure. Ma et al. [199] took 5300 oxyhalides from the periodic table to predict bandgap and the ML technique used were SVR, GBR, (GBR was the best); in their study, the model were taught via 300 octahedral oxyhalides. Then this model was cast-off to screen the residual 5000. The most trivial implementation of ML on computationally produced data is to screen the amount of data that is usually very large to invent novel and enhanced alternatives. The collection of data is done by combining elements in the periodic table, solved with little accuracy. Then one or more machine learning method is executed to analyze the data, which are trained with more accurate and smaller datasets. The summary of ML techniques based on computational data is shown in Table 5.

Based on experimental data, some experimentations associated with large datasets are very challenging; Some researchers augment the experimental results with computationally created data to conquer this problem. Pilania et al. [198] studied the estimation of formability of perovskites; they had taken 185 data points from [197], and support vector classification is used. 11 features dataset cast-off on behalf of the training model to foresee the formability. Li et al. [200] studied the optimization of materials compatibility, and to evaluate efficiency, the adopted ML techniques were ANN, LR, SVR, KNN, and RF, and then with the addition of some descriptors with bandgap, they predict cell performance. Odabasi & Yildirim [201] studied high-efficiency conditions and took 1921 efficiency data from 800 papers; they used ARM, DT, RF, and descriptive statistics. Descriptive statistics are used to analyze trends, factor effects are determined by ARM & DT, and RF is used for prediction. Oviedo et al. [202] performed a study to categorize data in dimensionality and space groups, XRD data (experimental) are augmented by computational ICSD data to train a-CNN based model to perform classification on dimensionality and space group. The data were in-house experimental XRD data (151 thin films). Hartano et al. [203] used SVR, LR, SVC, ANN, and KNN machine learning techniques to design an organic capping layer. The data are in-house for the capping layer (21 organic salts at 12 handling circumstances). In their study, modeling is done on 12 different conditions and stability. Capping layer is designed on 3D perovskite (with 21 organic layers). Odabasi et al. [204] studied ARM and pooled variance ML technique to predict stability, reproducibility relation, and hysteresis. 194 papers are used to

take 387 hysteresis data, and 24,142 reproducibility data are taken from 438 papers. The summary of ML techniques based on the experimental data set is tabulated in Table 6.

7. Stimuli affecting solar power forecast

PV power growth is witnessed in previous decades due to many factors like a consistent drop in manufacturing costs associated with PV systems, increased efficiency, low operational and maintenance cost, installation modularity, improved service life, and environment-friendly [205]. They are now competing with conventional sources of power generation (fossils) in several countries. It is instrumental in grid-connected modes, nevertheless, its workability finely depends on the ambient solar conditions. The solar incidence varies reliant on the geographical location, and also throughout the day, PV output is a function of the movement of sun, i.e., intensifying phase in the morning, maximized operation in the mid-day time, and falling with the dusk. This suggests PV output is vibrant in nature and depends on climate and location. The intensity of solar radiation diverges with geographical latitudes and longitudes, season, atmospheric condition, air quality, pollution index (fog and smog), etc. Currently, precise forecast of PV power is a vital research dome [206,207]. Variation n outputs of PV [205], these unpredictable outcomes considerably influence the stability, reliability, and scheduling of power system operation [208].

7.1. Solar power forecasting factors (PVPF)

Fig. 14.

Prediction of PVPF with accuracy is an erudite task; it rests on various aspects such as; (i) Horizons of forecasting, (ii) Weather classification, (iii) Forecast model performance, (iv) Forecast model inputs, (v) Timestamp as demonstrated in Fig. 15. This topic reviews the following PV Power forecasting factors.

7.1.1. Horizons of forecast

Forecast Horizon is the time interval amid actual and effective prediction time. i.e., it is the future period for output forecasting. Forecast Horizon is classified into three regimes; short-, medium-, and long-term [209,210]. Some researchers added one more ultra-short-term or concise term in the regime [205].

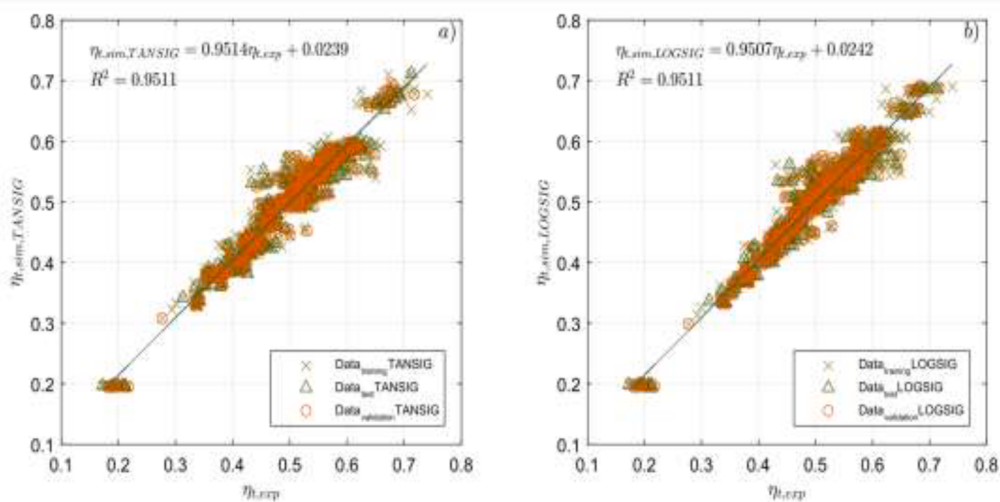
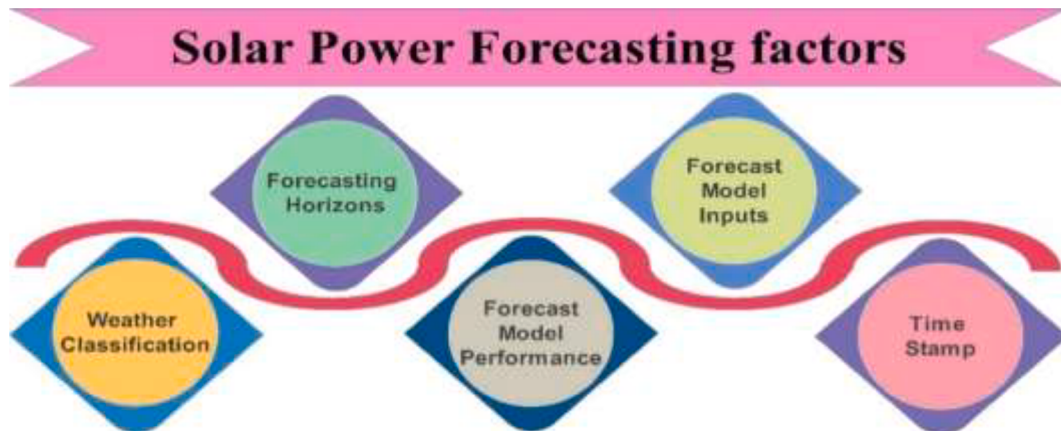
Table 5
Summary of ML techniques based on computational (DFT Generated) data set.

Aim	ML technique	Data source	Description	Refs.
Database construction for analysis.	Clustering (similarity analysis)	1346 HOIPs, (DFT)	DFT is used to calculate band gaps, dielectric constant, optimized structures, and energy. The model was recognized by experimental data.	Kim et al. [188]
Thermodynamic stability prediction.	CH, RF, ANN, DT, RR, Adaptive boosting	249,984 perovskites (periodic tables)	A convex hull is used for the calculation of stability. 2000 materials are used for training and others for testing.	Schmidtli et al. [189]
Ruddlesden Popper phases and bandgap prediction.	ANN	220 perovskites (periodic table)	Screening for radioactivity and octahedral factor of 220 perovskites with desirable tolerance.	Alam et al. [190]
For band prediction (screening).	GBR, SVM, KRR, MPR, DT (best is GBR)	5158 from periodic table	ML and DFT simulation of others are performed. Prediction of the bandgap of 5158 HOIP.	Lu et al. [191]
For band gap prediction screening.	RF	High throughout DFT (15,000 perovskites)	18 descriptors are used to anticipate the band gap. 10 stable perovskite having significant band gap is found.	Takahashi et al. [192]
Formability prediction.	SVM, weighted KNN	The materials project & ICSD (590-single, 538-double perovskite)	Formability analysis based on features (ionic radii, atomic number, electronegativity).	Xu et al. [193]
Screening of inorganic material.	KNN, GB, RF, MLP, GBDT, DT	JARVIS-DFT database (5097 material)	Screening was performed by spectroscopic partial maximum efficiency, effective carrier mass, and stability.	Chaudhari et al. [194]
Heat generation and bandgap formation prediction.	GBRT	540 double halide perovskites (periodic table)	GBRT used for the prediction of band gap and heat formation.	Im et al. [195]
Stability, structure and band gap screening.	SVM	454 DFT data	MP, AFLOW, OQMD are cast-off to choose material for DFT prediction.	Jain et al. [196]
Band gap prediction (material discovery).	GBR, SVR, RFR (best is GBR)	5300 oxyhalides (periodic Table 300-DFT data for training)	Model trained with 300 octahedral oxyhalides, for remaining ML model is used for screening.	Ma et al. [199]

Table 6

Summary of ML analysis based on experimental data.

Aim	ML technique	Data source	Description	Refs.
Formability prediction of perovskite.	SVC	Data points (185) from	11 feature datasets are cast-off for training SVC model, and they are cast-off to foresee the formability of 455 materials.	Pilania et al. [198]
To predict efficiency and material composition.	LR, ANN, SVR, KNN and RF	333 efficiency data	Bandgap is predicted from the material composition by ML, and then by bandgap and some descriptors cell performance is predicted.	Li et al. [200]
To determine high efficiency conditions.	ARM, DT, RF, descriptive statistics	Efficiency data (1921) from papers (800)	Trends are analyzed using descriptive statistics, ARM, and DT. RF for prediction.	Obadasi & Yildirim [201]
To classify data in space groups and dimensionality.	Different ML tools (best is CNN)	Experimental XRD data (in-house) for thin film	CNN model is trained by augmenting experimental data and computational ICSD data.	Oviedo et al. [202]
To design organic capping layer rationally.	KNN, SVR, GB, RF, ANN, LR	21 organic salts at 12 processing conditions	Capping layers are formed in perovskites (3D).	Hartono et al. [203]
To assess the relationship between stability, reproducibility, and hysteresis.	Pooled variance and ARM	24,142 reproducibility data and 387 hysteresis data from paper	ARM and pooled variance is done to analyze hysteresis data.	Obadasi & Yildirim [204]

**Fig. 14.** Experimental results against simulated ANN results [176]. Figure Reprinted with permission from Elsevier LN 5,547,030,951,595.**Fig. 15.** Solar PVPF factors.

- v Ultra short term forecast or concise-term forecast: this is used when the forecast period varies from seconds to less than 30 min [211]. Some researchers considered 1 min to one or numerous hours in this category. These forecasts are used for electricity pricing or making, power smoothing process, PV storage control etc. [212].
- v Short term forecast: In this, the temporal horizon is between 30 and 360 min [211]. But certain researchers considered one to some hours, one day, or up to 7 days in this regime [212]. It is mainly popular in the electricity market.
- v Medium term forecast: This regime spans 6–24 h [211]; however, some researchers examined one day, one week, and up to a month in

- this group. It is used for maintaining the schedule of solar energy integrated power systems [212].
- v Long term forecast: This regime predicts scenarios more than 24 h beforehand [211]. However, some have categorized periods of a month to a year in this regime [212]. These prediction horizons are appropriate for long-term power generation, transmission, distribution, and rationing of solar energy [213]. For seasonal trends account. But this type of model predicts fewer accuracy results due to weather fluctuations.

There is a complexity due to different time horizons. Several investigators establish a forecast horizons classification approach, especially for PV Power forecasting (PVPF): intra-hour, intra-day, and day ahead. Sometimes these groups overlap with the short, medium, and long-term groups/ category.

- v Intra-hour: It is also called nowcasting; forecast horizons are taken from a few seconds to hour [214] (it overlaps with very short term horizon categories). Grid quality as well as the stability is firmly ensured in these types of forecasts.
- v Intra-day: This forecast usually overlaps with short term forecast and medium-term forecast. The temporal horizon span 1–6 hour.
- v Day ahead: In this regime, forecast spans 6–48 h overlaps with medium- and long-term horizons. Models in utility planning and unit commitment use such type of model.

Almonacid et al. [215] introduced a PVPF intraday using Artificial Neural Network; their study accurately predicts 1 hour ahead PV output, the inputs were the global horizontal Irradiance (GHI) and cell temperature. Two non-linear auto-regression models are used for these two inputs, which predict the cell temperature and GHI. The normalized root means square error (nRMSE) of obtained cell temperature with ANN based was 3.33%. Zhang et al. [216] studied intra-day and day-ahead combined forecast horizons. They studied four scenarios on the basis of the geographical location and collection obtained sound forecasts with nRMSE (range- 2–17%) and a huge ensemble of PV systems (64 and 495GW). Day-ahead forecast frequently uses NWP output because NWP improves accuracy when the time horizon increases. There are limited studies for more extended forecast prediction.

7.1.2. Weather classification

PV output depends intensely on meteorological impact factors like; direction and wind speed, distribution of aerosol, cloud cover, humidity etc. thus, changed weather status will affect the accuracy of PVPF. Thus, models should integrate weather classification with forecasting for improved robustness of the PVPF models. PVPF model based on weather classification faces difficulties of insufficient training data sets. Some authors classified the 33 standard meteorological weather categories into 10 single new weather type [62], and some researcher has categorized them into less than 4 types [62,68,217].

Wang et al. [62] studied the PVPF model separately for each weather class, improving mapping and forecast prediction [62,218,219]. They used Generative Adversarial Network (GAN) and augmented it with a convolutional neural network (CNN), and the authors suggest that the GAN—CNN PVPF model based on day-ahead was more accurate. For a researcher, the proper selection of PVPF models in weather classification is tough. The authors studied [62] comparing their GAN-based weather classification approach with 10 weather classes and 5 recognized forecast models. A confusion matrix is studied for objectivity [220]. This tool visualizes algorithms (classifier algorithm), and performance (for comparison). Three indices calculate the performance: PA (product accuracy), UA (users accuracy), and OA (overall accuracy). The standard classifier equated were: CNN with 1D convolutional layer (CNN 1D), CNN with 2D convolutional layer (CNN 2D), multi-layer perceptron (MLP), and SVM and k-nearest neighbor (KNN). CNN 2D performed the best for all non-linear input-output relationships. So, the authors

endorsed GAN—CNN 2D for PVPF modeling.

7.1.3. Forecast model performance

For evaluating models forecast accuracy, it is necessary to estimate performance. These take account of Mean Absolute Error (MAE), Mean Absolute Percentage Error (MAPE), and root Mean Square Error (RMSE) [65,66]; the Table 7 below gives a briefing of these;

7.1.4. Forecast model inputs

It seems the direct influence of inputs of forecasting models on prediction accuracy. These are often vital factors in shaping model performance. Imprudent selection of inputs often causes forecast errors which surges cost, time delay, and computational complexity. The inputs required for the PV system are mainly meteorological parameters like; solar irradiance, temperature, ambient temperature, wind velocity, module temperature and humidity [221], barometric pressure [218, 219,222], and aerosol properties [223–226]. All these input variables depend on climatic and geographical conditions.

7.1.5. Time stamp

The time stamp factor plays a significant part in predicting the PVPF model's accuracy. The time stamp introduces uncertainty in the forecast [227]. It is reliable in midday as compared to morning and dusk evening. In addition, these uncertainties in power estimation vary depending on locations and seasons. ANN is used [227] for modeling PVPF as the model can elucidate input or output relations like a time stamp and weather data and PV output.

7.2. Forecasting techniques by machine learning

The methods depend on Artificial Intelligence's ability to learn from the experiences with some datasets and further predict the required output via several trials runs. In this regime, powerful computations are essential to run several iterations beforehand the final predictions. This has many applications like; classification problems, filtering, forecasting, pattern recognition and data mining. The section discusses the following techniques, which are widely used for PV power forecasting. Multi-layer perceptron neural network (MLPNN), Recurrent neural network (RNN), Feed-forward neural network (FFNN), Extreme learning machine (ELM) and Feedback neural network (FBNN) [41]. These are discussed in later sections.

ANN resembles the evidence handing out the mechanism of the humanoid brain. Although ANN has been discussed in previous sections, it is finely capable of solving non-linear functions with very high accuracy. It has been widely used in various arenas of meteorological predictions,

Table 7
Briefing of forecast models.

Tools	Description	Equations
Mean Absolute Error (MAE)	Calculates models uniform forecast error.	$MAE = \frac{1}{N} \sum_{i=1}^N y_i - t_i $
Root Mean Square Error (RMSE)	Overall accuracy is measured. Square increases the prediction error rate.	$RMSE = \sqrt{\frac{1}{N} \sum_{i=1}^N y_i - t_i ^2}$
Normalized Root Mean Square Error (nRMSE)	Calculates overall accuracy in huge datasets. Square boost the prediction error rate.	$nRMSE = \frac{\sqrt{\sum_{i=1}^N (y_i - t_i)^2}}{\sqrt{\sum_{i=1}^N y_i^2}}$
Mean Absolute Percentage Error (MAPE)	Calculates reliable forecasting error in percentage.	$MAPE = \frac{1}{N} \sum_{i=1}^N \frac{ y_i - t_i }{y_i} \times 100\%$
Normalized Mean Absolute Percentage Error (nMAPE)	Calculates reliable forecasting error in percentage. Used for large datasets.	$nMAPE = \frac{1}{N} \sum_{i=1}^N \frac{ y_i - t_i }{\frac{1}{N} \sum_{i=1}^N y_i} \times 100\%$

engineering, finance, physics, medicine, etc. Some of the recent modifications that have occurred in the past few decades will be discussed in this section:

7.2.1. Multi-layer perceptron neural network (MLPNN)

From the perspective of basic understanding of the architecture and working MLPNN is studied in Section 2.4.3. MLPNN could be considered the benchmark as opined by some researchers [228,229]. Hegazy et al. [230] studied that a single layer is capable of a non-linear function having an adequate number of nodes. Also, if the number of nodes is too much, there will be difficulties like overfitting [231].

7.2.2. Recurrent neural network

The section is above discussed in the deep learning Section 3.1 as other related techniques require acquaintance with the algorithm there, this section, keenly focus on the PV forecast by RNN. RNN can acquire and practice very complicated and compound relationships and computational structures. It is a noticeable class of ANN. RNN depends on time series data by a feedback system to inherit previous time step values. The model has a feedback loop with simple structures, which makes it work as a forecasting engine. The apprehensive neural layer's output is added with the following input vector and feedback to the same layer. Elman et al. [232] highlighted the study where the architecture has a feedback loop that communicates with hidden layers of the network and input layers. These feedback loops tend to diminish learning errors. Williams and Zipser [233] studied a series of experiments to analyze the learning rates of the model.

7.2.3. Radial basis function neural network (RBFNN)

As compared with other ANN approaches RBFNN seems to be better and quicker. Hence in time series predictions, approximation, classification, and system control, RBFNN is mainly used. The activation function is the Radial Basis Function. There are two layers in this model. The characteristics are added with RB activation function in the first layer itself. Then, the output of the first layer computes the next time step's output. Both layers are introduced with their weights. Input information is used to generate the first layer weight while the second layer's weight is to be calculated.

7.2.4. Extreme learning machine

ELM is mainly used for single-layer feed-forward networks (SLFN) also, ELM is an advanced data-driven method [234]. ELM networks have enumerated capacity and descent algorithms having fewer training errors and weights. Thus ELM has faster learning speeds and easy to implement as compared to traditional ANNs [235]. Also, ELM is mostly preferred as easier algorithms requiring less training input data. Al-David, et al. [234] studied ELM for PVPF due to model simplicity. The network structure has an input layer, hidden layer, and output layer.

The network equation is given by Eq. (29):

$$y_i = \sum_{j=1}^K \beta_j g(w_j x_i + b_j), \quad j = 1, 2, \dots, N \quad (29)$$

Where w_i and β_1 are input and output neurons weight vector of i th hidden layer, respectively. b_i is bias of network.

The simplified matrix representation of the above equation is as:

If the training set numbers in the sample are equal to the number of hidden layers ($y_i = t_i$) [236].

$$H\beta = T \quad (30)$$

The output matrix of hidden layer H is given by Eq. (31) and (32):

$$H = \begin{bmatrix} h_{(x1)} \\ \vdots \\ h_{(xn)} \end{bmatrix} = \begin{bmatrix} \dots & g(w_1 x_1 + b_1) & \dots & g(w_k x_1 + b_k) \\ \dots & g(w_1 x_1 + b_1) & \dots & g(w_k x_k + b_k) \end{bmatrix}_{N \times K} \quad (31)$$

$$\beta = \begin{bmatrix} \beta_1 \\ \vdots \\ \beta_K \end{bmatrix}_{K \times m} \quad T = \begin{bmatrix} T_1 \\ \vdots \\ T_k \end{bmatrix}_{m \times 1} \quad (32)$$

Where β and T are output vector and expected target, respectively.

Hossain et al. [237] studied an alternative ELM model that exhibits great forecast accurateness and learning rate capacity as related to SVR and ANN. Some authors [238] mentioned the PVPF model's accuracy with ELMs or echo state networks. Some of the works on the forecast of solar power is suggested in the Table 8.

8. Conclusion

This review presents the adoption of machine learning in solar energy generation, and for that, the authors had reviewed nanofluids in solar devices and the prognosis of solar power; the concluding points are as follows:

- DL comes under the regime of unsupervised ML technique having hierarchical representation at several layers providing automatic learning features, most suitable for dealing with complex problems and extensive data. The method is exceptionally scalable in terms of computation and data.
- Thermophysical properties, thermal performance of heat exchanger, and nanofluid performance in solar energy systems are studied by various ML methods due to various factors and their non-linear effects that make nanofluid research complications. Strong artificial intelligence is hardly practical in these complicated problems ML can be cost-effective and very useful in nanofluid research.
- Various aspects affect the thermophysical properties of nanofluids. Empirical correlations and theoretical analysis are subjected to significant uncertainties. ML methods, including ANN give excellent judgment of nanofluid properties.
- ML techniques such as ANN and ANN-GA have been found effective in predicting exergy efficiency, heat transfer, and pressure drop in heat exchangers. Nanofluids, with their high thermal conductivity, are widely used in solar collectors and PV/T systems.
- The integrated ANN with intelligence algorithms would advance prediction accurateness. The PAC learning justifies the sample size and tests the learnability of a specific machine algorithm.
- Transfer learning is advantageous for the ML application in Perovskite solar cells.
- The fluctuating environment of solar irradiance affects the dependency of the photovoltaics incorporated system. This penetration of radiance into the collecting device leads to variation in voltage and power fluctuations. For this reliable forecasting is meant and is the solution, it can be classified over a range of ultra-short term to long term.
- Although the predictions are pretty good, exact forecasts are puzzling, and desperate methods consisting of statistical, physical, and hybrid models are investigated. In which ANN, especially CNN and its hybrid, are most promising for forecast accuracy.
- Designing useful PVPF model performance estimation, forecast horizons, inputs and pre-processing optimization, timestamp, uncertainty quantification, and weather classification must be considered.
- In general, forecast errors are more significant in longer forecast horizons. Improper inputs can cause more errors leading to time delay, computational complexity, and cost overrun. Among specific inputs, solar irradiance is associated with PV output. GA and PSO have gained importance in the optimization of network parameters such as weights and biases.

The current study domain discussed in the manuscript has ample opportunities for further exploration, particularly in the area of solar devices with power prediction and heat transfer fluid property evaluation. The author recommends further research on the application of

Table 8
ANN based forecasting technique.

Model	Forecast horizon	Description	Input data	Pre-processing of data	Accuracy	Refs.
LSTM	Hourly	LSTM improves day-ahead irradiance prediction performance over FFNN, BPNN, and LISR models.	Wind speed, visibility, weather type, temperature, humidity, dew point.	Normalized	18.34% RMSE	Qing and Niu et al. [46]
WNN	Hourly	Morlet and Mexican hat type function (Activation function) is introduced for WT and feed-forward ANN model. The results are superior as equated with ETS, ARIMA, and ANN.	Solar irradiance	Wavelet transform	9.42 – 15.41% nRMSE	Sharma et al. [239]
KNN and ANNs	15 min 2 h	Global solar irradiance forecasting is done by combining ANN model with KNN. Time horizon from 15 min to 2 h. The method yields better results than a simple forecasting scheme.	Cloud pattern, sky clarity, and GSI.	Normalize	RMSE (%) < 15	Pedro and Coimbra et al. [240]
MLR, FFNN and GRNN	24 h	GRNN was integrated with hybrid MLR and FFNN, and the model forecast PV power output.	Temperature, wind speed, atmospheric pressure, wind direction, sunshine hours, solar irradiance.	Normalize	2.74% RMSE	Ramsami and Orea et al. [241]
ANN	24 h	ANN model was studied to predict day-ahead PV output. Aerosol index is used as an input and correlated with solar incident radiation. This model is better than conventional ANN.	Temperature, wind speed, Aerosol Index (AI), and humidity.	Normalize	11% MAE	Liu et al. [242]
RBFNN	24 h	RBFNN model is developed with data regularity scheme for PV output forecasting.	2 days of calculated PV power generation data in time series form.		3.71 MAPE (%) and 4.65 RMSE (%)	Lu and chang et al. [243]
ANN Levenberg Marquardt Back-Propagation algorithm	0–45 min	The algorithm optimized the weights of ANN to obtain the best input-response mapping.	PV panel (750 Wp) cell and ambient temperature diffuse irradiation (solar).		RMSE = 19.9515 – 54.11052	Izgi et al. [244]
ANN	5 min	Using horizontal solar radiation inputs can address the absence of tilted solar radiation data and eliminate the need for an inclined pyranometer after sufficient model training.	Solar declination, azimuth angle, horizontal irradiance, zenith angle, and extraterrestrial irradiance.		8.81% RMSE	Dahmani et al. [245]
ANN	Seasonal forecast	High accuracy forecast is generated by pre-processed data into optimized ANN algorithm.	Daily solar irradiance (global) data	Normalized	nRMSE < 2%	Paoli et al. [246]
Fuzzy logic & ANN	Monthly	For solar power estimation, ANN is coupled with multi-layer BP and fuzzy pre-processing approach. The algorithm's performance is better than ANN & hybrid ANN-fuzzy models.	Wind speed, dew point, gust wind, temperature, solar irradiance.	Fuzzy pre-processing toolbox	29.6% MAPE	Sivaneasan et al. [247]
GA optimized ANN	5, 10 and 15 min	A GA optimized scheme is introduced for real time output forecasting of 48 MWe PV plant. Model gives better results than ARMA and kNN models.	Clear sky index, solar irradiance, cloud position, solar output power.	Pseudo-cartesian transform	21.02 MAE (%)	Chu et al. [248]
PSO-GA and ANN		ANN model is optimized using PSO-GA to forecast the performance of SSHS.	Solar radiation, water temperature (storage tank), ambient temperature, outlet temperature (PTC).	normalized	RMSE < 24%	Jamali et al. [249]
Neural network with the statistical method	1 week	PV power output forecasting can be approached through either physical or statistical methods, with the former relying on system construction and the latter utilizing neural network models trained on historical data.	Air temperature, position, cloud, and humidity of sun, solar irradiance.		10% and 13% nRMSE	Huang, et al. [250]

machine learning in hybrid renewable energy systems such as solar and wind, solar and tidal, etc. and implementing machine learning tools with solar-based power cycles such as the Kalina cycle or Organic Rankine Cycle. Additionally, the authors faced challenges in locating experimental data, particularly in the field of nanofluid properties. Thus, it is recommended to develop more comprehensive experimental studies for nanofluids with different types of nanoparticles and base fluids. Machine learning can be combined with other technologies such as IoT, cloud computing, and blockchain to develop more powerful applications. Future studies can focus on exploring the integration of machine learning with other technologies to develop new applications.

Declaration of Competing Interest

The authors declare that they have no known competing financial interests or personal relationships that could have appeared to influence the work reported in this paper.

Data availability

No data was used for the research described in the article.

References

- [1] Parvin H, et al. A new classifier ensemble methodology based on subspace learning. *J Exp Theor Artif Intell* 2013;25(2):227–50.
- [2] Minaei-Bidgoli B, et al. Effects of resampling method and adaptation on clustering ensemble efficacy. *Artif Intell Rev* 2014;41(1):27–48.
- [3] Ryu JW, Kantardzic M, Walgampaya C. Ensemble classifier based on misclassified streaming data. In: Proceedings of the 10th IASTED international conference on artificial intelligence and applications; 2010.
- [4] Sarvaiya JN, Pandey PC, Pandey VK. An impedance detector for glottography. *IETE J Res* 2009;55(3):100–5.
- [5] Parvin H, MirnabiBaboli M, Alinejad-Rokny H. Proposing a classifier ensemble framework based on classifier selection and decision tree. *Eng Appl Artif Intell* 2015;37:34–42.
- [6] Ahmad A, Dey L. A k-mean clustering algorithm for mixed numeric and categorical data. *Data Knowl Eng* 2007;63(2):503–27.

- [7] Tran MQ, et al. Experimental setup for online fault diagnosis of induction machines via promising IoT and machine learning: towards industry 4.0 empowerment. *IEEE Access* 2021;9:115429–41.
- [8] Elsisi M, et al. Effective IoT-based deep learning platform for online fault diagnosis of power transformers against cyberattack and data uncertainties. *Measurement* 2022;110686.
- [9] Ismail MM, Bendary AF, Elsisi M. Optimal design of battery charge management controller for hybrid system PV/wind cell with storage battery. *Int J Power Energy Convers* 2020;11(4):412–29.
- [10] Zhao N, Li S, Yang J. A review on nanofluids: data-driven modeling of thermalphysical properties and the application in automotive radiator. *Renew Sustain Energy Rev* 2016;66:596–616.
- [11] Ramezanizadeh M, et al. A review on the utilized machine learning approaches for modeling the dynamic viscosity of nanofluids. *Renew Sustain Energy Rev* 2019;114:109345.
- [12] Bahiraei M, Heshmatian S, Moayedi H. Artificial intelligence in the field of nanofluids: a review on applications and potential future directions. *Powder Technol* 2019;353:276–301.
- [13] Alpaydin E. Introduction to machine learning. 3rd ed. MIT Press; 2014.
- [14] Larose DT, Larose CD. Discovering knowledge in data: an introduction to data mining. 4. John Wiley & Sons; 2014.
- [15] Jain A, et al. New opportunities for materials informatics: resources and data mining techniques for uncovering hidden relationships. *J Mater Res* 2016;31(8):977–94.
- [16] Ward L, et al. A general-purpose machine learning framework for predicting properties of inorganic materials. *npj Comput Mater* 2016;2(1):1–7.
- [17] Butler KT, et al. Computational materials design of crystalline solids. *Chem Soc Rev* 2016;45(22):6138–46.
- [18] Mellit A, Kalogirou S. Artificial intelligence and internet of things to improve efficacy of diagnosis and remote sensing of solar photovoltaic systems: challenges, recommendations and future directions. *Renew Sustain Energy Rev* 2021;143:110889.
- [19] Tukey, J.W., Exploratory data analysis as part of a large whole. 1973.
- [20] Schmack R, et al. A meta-analysis of catalytic literature data reveals property-performance correlations for the OCM reaction. *Nat Commun* 2019;10(1):1–10.
- [21] Helal S. Subgroup discovery algorithms: a survey and empirical evaluation. *J Comput Sci Technol* 2016;31(3):561–76.
- [22] Goldsmith BR, et al. Uncovering structure-property relationships of materials by subgroup discovery. *New J Phys* 2017;19(1):013031.
- [23] Ottman N, et al. Soil exposure modifies the gut microbiota and supports immune tolerance in a mouse model. *J Allergy Clin Immunol* 2019;143(3):1198–206. e12.
- [24] Zendehboudi A, Li X. Robust predictive models for estimating frost deposition on horizontal and parallel surfaces. *Int J Refrig* 2017;80:225–37.
- [25] Du KL, Swamy MN. Neural networks in a softcomputing framework. Springer Science & Business Media; 2006.
- [26] Ma T, et al. Recent trends on nanofluid heat transfer machine learning research applied to renewable energy. *Renew Sustain Energy Rev* 2021;138:110494.
- [27] Anastasakis, L. and N. Mort, The development of self-organization techniques in modelling: a review of the group method of data handling (GMDH). Research report-university of sheffield department of automatic control and systems engineering, 2001.
- [28] Ahmadi MH, et al. Applying GMDH neural network to estimate the thermal resistance and thermal conductivity of pulsating heat pipes. *Eng Appl Comput Fluid Mech* 2019;13(1):327–36.
- [29] Mulashani AK, et al. Enhanced group method of data handling (GMDH) for permeability prediction based on the modified Levenberg Marquardt technique from well log data. *Energy* 2022;239:121915.
- [30] Tang J. ANFIS: adaptive network based fuzzy inference systems. *IEEE Trans Syst Cybern* 1993;23:515–20.
- [31] Zendehboudi A, Tatar A. Utilization of the RBF network to model the nucleate pool boiling heat transfer properties of refrigerant-oil mixtures with nanoparticles. *J Mol Liq* 2017;247:304–12.
- [32] Ahmad MW, Reynolds J, Rezgui Y. Predictive modelling for solar thermal energy systems: a comparison of support vector regression, random forest, extra trees and regression trees. *J Clean Prod* 2018;203:810–21.
- [33] Suykens JA, Vandewalle J. Recurrent least squares support vector machines. *IEEE Trans Circuits Syst I Fundam Theory Appl* 2000;47(7):1109–14.
- [34] Gestel T, van, Suykens JAK, Baesens B, Viaene S, Vanthienen J, Dedene G, De Moor B, Vandewalle J. Benchmarking least squares support vector machine classifiers. *Mach Learn* 2004;54(1):5–32.
- [35] Ahmadi MA, Ebadi M. Evolving smart approach for determination dew point pressure through condensate gas reservoirs. *Fuel* 2014;117:1074–84.
- [36] Suykens JA, Vandewalle J. Training multilayer perceptron classifiers based on a modified support vector method. *IEEE Trans Neural Netw* 1999;10(4):907–11.
- [37] Deng L, Yu D. Deep learning for signal and information processing. Microsoft Res Monogr 2013.
- [38] Hinton GE, Osindero S, Teh YW. A fast learning algorithm for deep belief nets. *Neural Comput* 2006;18(7):1527–54.
- [39] MacKay DM, McCulloch WS. The limiting information capacity of a neuronal link. *Bull Math Biophys* 1952;14(2):127–35.
- [40] Kumari P, Toshniwal D. Deep learning models for solar irradiance forecasting: a comprehensive review. *J Clean Prod* 2021;318:128566.
- [41] Ahmed R, et al. A review and evaluation of the state-of-the-art in PV solar power forecasting: techniques and optimization. *Renew Sustain Energy Rev* 2020;124:109792.
- [42] Hüskens M, Stagge P. Recurrent neural networks for time series classification. *Neurocomputing* 2003;50:223–35.
- [43] Yu C, et al. A novel framework for wind speed prediction based on recurrent neural networks and support vector machine. *Energy Convers Manage* 2018;178:137–45.
- [44] Rahman A, Srikumar V, Smith AD. Predicting electricity consumption for commercial and residential buildings using deep recurrent neural networks. *Appl Energy* 2018;212:372–85.
- [45] Bandara K, Bergmeir C, Smilj S. Forecasting across time series databases using recurrent neural networks on groups of similar series: a clustering approach. *Expert Syst Appl* 2020;140:112896.
- [46] Qiao X, Niu Y. Hourly day-ahead solar irradiance prediction using weather forecasts by LSTM. *Energy* 2018;148:461–8.
- [47] Yue W, et al. Machine learning with applications in breast cancer diagnosis and prognosis. *Designs* 2018;2(2):13.
- [48] Xie C, et al. Cross-correlation conditional restricted Boltzmann machines for modeling motion style. *Knowl Based Syst* 2018;159:259–69.
- [49] Papa JP, et al. Model selection for discriminative restricted boltzmann machines through meta-heuristic techniques. *J Comput Sci* 2015;9:14–8.
- [50] Tang Y, Salakhutdinov R, Hinton G. Robust boltzmann machines for recognition and denoising. In: Proceedings of the IEEE conference on computer vision and pattern recognition. IEEE; 2012.
- [51] Hinton GE, et al. The "wake-sleep" algorithm for unsupervised neural networks. *Science* 1995;268(5214):1158–61.
- [52] Nair V, Hinton GE. 3D object recognition with deep belief nets. *Adv Neural Inf Process Syst* 2009;22:1339–47.
- [53] Deng L, Yu D, Platt J. Scalable stacking and learning for building deep architectures. In: Proceedings of the IEEE international conference on acoustics, speech and signal processing (ICASSP). IEEE; 2012.
- [54] Arel I, Rose DC, Karnowski TP. Deep machine learning-a new frontier in artificial intelligence research [research frontier]. *IEEE Comput Intell Mag* 2010;5(4):13–8.
- [55] Liao B, et al. An image retrieval method for binary images based on DBN and softmax classifier. *IETE Tech Rev* 2015;32(4):294–303.
- [56] Deng L. Three classes of deep learning architectures and their applications: a tutorial survey. *APSIPA Trans Signal Inf Process* 2012.
- [57] Fukushima K, Miyake S, Ito T. Neocognitron: a neural network model for a mechanism of visual pattern recognition. *IEEE Trans Syst Man Cybern* 1983;(5):826–34.
- [58] Jiang X, et al. Cascaded subpatch networks for effective CNNs. *IEEE Trans Neural Netw Learn Syst* 2017;29(7):2684–94.
- [59] Gu J, et al. Recent advances in convolutional neural networks. *Pattern Recognit* 2018;77:354–77.
- [60] Zang H, et al. Short-term global horizontal irradiance forecasting based on a hybrid CNN-LSTM model with spatiotemporal correlations. *Renew Energy* 2020;160:26–41.
- [61] Wang Y, Li H. A novel intelligent modeling framework integrating convolutional neural network with an adaptive time-series window and its application to industrial process operational optimization. *Chemos Intell Lab Syst* 2018;179:64–72.
- [62] Wang F, et al. Generative adversarial networks and convolutional neural networks based weather classification model for day ahead short-term photovoltaic power forecasting. *Energy Convers Manage* 2019;181:443–62.
- [63] Eigen, D., et al., Understanding deep architectures using a recursive convolutional network. arXiv preprint arXiv:1312.1847, 2013.
- [64] Desjardins G, Bengio Y. Empirical evaluation of convolutional RBMs for vision. DIRO Univ Montr 2008:1–13.
- [65] Hu Q, Zhang R, Zhou Y. Transfer learning for short-term wind speed prediction with deep neural networks. *Renew Energy* 2016;85:83–95.
- [66] Qureshi AS, et al. Wind power prediction using deep neural network based meta regression and transfer learning. *Appl Soft Comput* 2017;58:742–55.
- [67] Yang HT, et al. A weather-based hybrid method for 1-day ahead hourly forecasting of PV power output. *IEEE Trans Sustain Energy* 2014;5(3):917–26.
- [68] Chen C, et al. Online 24-h solar power forecasting based on weather type classification using artificial neural network. *Sol Energy* 2011;85(11):2856–70.
- [69] Gao Y, Miyata S, Akashi Y. Multi-step solar irradiation prediction based on weather forecast and generative deep learning model. *Renew Energy* 2022;188:637–50.
- [70] Wang F, et al. A day-ahead PV power forecasting method based on LSTM-RNN model and time correlation modification under partial daily pattern prediction framework. *Energy Convers Manage* 2020;212:112766.
- [71] Zadeh PM, et al. Hybrid optimization algorithm for thermal analysis in a solar parabolic trough collector based on nanofluid. *Energy* 2015;82:857–64.
- [72] Freuder EC. In pursuit of the holy grail. *Constraints* 1997;2(1):57–61.
- [73] Gu J, et al. Algorithms for the satisfiability (SAT) problem: a survey. Cincinnati Univ oh Dept of Electrical and Computer Engineering; 1996.
- [74] Brewka G, Eiter T, Truszczynski M. Answer set programming at a glance. *Commun ACM* 2011;54(12):92–103.
- [75] Apt K. Principles of constraint programming. Cambridge University Press; 2003.
- [76] Fleischanderl G, et al. Configuring large systems using generative constraint satisfaction. *IEEE Intell Syst Their Appl* 1998;13(4):59–68.
- [77] Carbonell JG, Michalski RS, Mitchell TM. Machine learning: a historical and methodological analysis. *AI Mag* 1983;4(3):69, 69.
- [78] Gent, I., et al., Machine learning for constraint solver design-A case study for the alldifferent constraint. arXiv preprint arXiv:1008.4326, 2010.

- [79] Wang CJ, Tsang EP. Solving constraint satisfaction problems using neural networks. In: Proceedings of the S international conference on artificial neural networks. IET; 1991.
- [80] Adorf HM, Johnston MD. A discrete stochastic neural network algorithm for constraint satisfaction problems. In: Proceedings of the IJCNN international joint conference on neural networks. IEEE; 1990.
- [81] Arbelaez A, Hamadi Y, Sebag M. Continuous search in constraint programming, in autonomous search. Springer; 2011. p. 219–43.
- [82] Galassi A, et al. Model agnostic solution of csp via deep learning: a preliminary study. In: Proceedings of the international conference on the integration of constraint programming, artificial intelligence, and operations research. Springer; 2018.
- [83] Bello, I., et al., Neural combinatorial optimization with reinforcement learning. arXiv preprint arXiv:1611.09940, 2016.
- [84] Lagoudakis MG, Littman ML. Learning to select branching rules in the DPLL procedure for satisfiability. *Electronic Notes Discrete Math* 2001;9:344–59.
- [85] Lederman G, et al. Learning heuristics for quantified boolean formulas through reinforcement learning. In: Proceedings of the international conference on learning representations; 2019.
- [86] Xu Y, Stern D, Samulowitz H. Learning adaptation to solve constraint satisfaction problems. In: Proceedings of the learning and intelligent optimization (LION); 2009.
- [87] Popescu A, et al. An overview of machine learning techniques in constraint solving. *J Intell Inf Syst* 2021;1:28.
- [88] Cappart, Q., et al., Combining reinforcement learning and constraint programming for combinatorial optimization. arXiv preprint arXiv:2006.01610, 2020.
- [89] Korte B, Vygen J. The knapsack problem, in combinatorial optimization. Springer; 2000. p. 397–406.
- [90] Guerri A, Milano M. Learning techniques for automatic algorithm portfolio selection. ECAI 2004.
- [91] Bonfietti A, Lombardi M, Milano M. Embedding decision trees and random forests in constraint programming. In: Proceedings of the international conference on integration of constraint programming, artificial intelligence, and operations research. Springer; 2015.
- [92] Hutter F, et al. Performance prediction and automated tuning of randomized and parametric algorithms. In: Proceedings of the international conference on principles and practice of constraint programming. Springer; 2006.
- [93] De Raedt L, Passerini A, Teso S. Learning constraints from examples. In: Proceedings of the AAAI conference on artificial intelligence; 2018.
- [94] Zhang, W., et al., NLocalSAT: boosting local search with solution prediction. arXiv preprint arXiv:2001.09398, 2020.
- [95] Selsam, D., et al., Learning a SAT solver from single-bit supervision. arXiv preprint arXiv:1802.03685, 2018.
- [96] Gebser M, et al. A portfolio solver for answer set programming: preliminary report. In: Proceedings of the international conference on logic programming and nonmonotonic reasoning. Springer; 2011.
- [97] Yang Z, Ishay A, Lee J. Neurasp: embracing neural networks into answer set programming. In: Proceedings of the 29th international joint conference on artificial intelligence (IJCAI 2020); 2020.
- [98] Karimipour A, et al. A novel nonlinear regression model of SVR as a substitute for ANN to predict conductivity of MWCNT-CuO/water hybrid nanofluid based on empirical data. *Physica A* 2019;521:89–97.
- [99] Nafchi PM, Karimipour A, Afrand M. The evaluation on a new non-Newtonian hybrid mixture composed of TiO₂/ZnO/EG to present a statistical approach of power law for its rheological and thermal properties. *Physica A* 2019;516:1–18.
- [100] Moradikazerouni A, et al. Assessment of thermal conductivity enhancement of nano-antifreeze containing single-walled carbon nanotubes: optimal artificial neural network and curve-fitting. *Physica A* 2019;521:138–45.
- [101] Bellos E, Tzivanidis C, Tsimpoukis D. Enhancing the performance of parabolic trough collectors using nanofluids and turbulators. *Renew Sustain Energy Rev* 2018;91:358–75.
- [102] Raj P, Subudhi S. A review of studies using nanofluids in flat-plate and direct absorption solar collectors. *Renew Sustain Energy Rev* 2018;84:54–74.
- [103] Kumar Singh S, Tiwari AKumar, Paliwal HK. A holistic review of MXenes for solar device applications: synthesis, characterization, properties and stability. *FlatChem* 2023;39:100493.
- [104] Ma T, et al. Recent trends on nanofluid heat transfer machine learning research applied to renewable energy. *Renew Sustain Energy Rev* 2020;110494.
- [105] Sidik NAC, Yazid MNAWM, Samion S. A review on the use of carbon nanotubes nanofluid for energy harvesting system. *Int J Heat Mass Transf* 2017;111:782–94.
- [106] Xu G, et al. A novel method to measure thermal conductivity of nanofluids. *Int J Heat Mass Transf* 2019;130:978–88.
- [107] Aparna Z, et al. Thermal conductivity of aqueous Al₂O₃/Ag hybrid nanofluid at different temperatures and volume concentrations: an experimental investigation and development of new correlation function. *Powder Technol* 2019;343:714–22.
- [108] Li F, et al. Effects of ultrasonic time, size of aggregates and temperature on the stability and viscosity of Cu-ethylene glycol (EG) nanofluids. *Int J Heat Mass Transf* 2019;129:278–86.
- [109] Esfe MH, Bahraei M, Mahian O. Experimental study for developing an accurate model to predict viscosity of CuO-ethylene glycol nanofluid using genetic algorithm based neural network. *Powder Technol* 2018;338:383–90.
- [110] Sarsam WS, et al. Stability and thermophysical properties of non-covalently functionalized graphene nanoplatelets nanofluids. *Energy Convers Manage* 2016;116:101–11.
- [111] Akilu S, et al. Viscosity, electrical and thermal conductivities of ethylene and propylene glycol-based β-SiC nanofluids. *J Mol Liq* 2019;284:780–92.
- [112] Khodadadi H, Toghraie D, Karimipour A. Effects of nanoparticles to present a statistical model for the viscosity of MgO-Water nanofluid. *Powder Technol* 2019;342:166–80.
- [113] Esfe MH, et al. Viscosity and rheological properties of antifreeze based nanofluid containing hybrid nano-powders of MWCNTs and TiO₂ under different temperature conditions. *Powder Technol* 2019;342:808–16.
- [114] Cai Y, Nan Y, Guo Z. Enhanced absorption of solar energy in a daylighting louver with Ni-water nanofluid. *Int J Heat Mass Transf* 2020;158:119921.
- [115] Markham IS, Rakes TR. The effect of sample size and variability of data on the comparative performance of artificial neural networks and regression. *Comput Oper Res* 1998;25(4):251–63.
- [116] Thomas RM, et al. Dealing with missing data, small sample sizes, and heterogeneity in machine learning studies of brain disorders. *Machine learning*. Elsevier; 2020. p. 249–66.
- [117] Moghaddam DD, et al. The effect of sample size on different machine learning models for groundwater potential mapping in mountain bedrock aquifers. *Catena* 2020;187:104421.
- [118] Selimfendigil F, Öztop HF. Thermoelectric generation in bifurcating channels and efficient modeling by using hybrid CFD and artificial neural networks. *Renew Energy* 2021;172:582–98.
- [119] Apolloni B, Gentile C. Sample size lower bounds in PAC learning by algorithmic complexity theory. *Theor Comput Sci* 1998;209(1–2):141–62.
- [120] Sheih G. Precise confidence intervals of regression-based reference limits: method comparisons and sample size requirements. *Comput Biol Med* 2017;91:191–7.
- [121] Longo GA, et al. Application of artificial neural network (ANN) for the prediction of thermal conductivity of oxide–water nanofluids. *Nano Energy* 2012;1(2):290–6.
- [122] Toghraie D, et al. Designing an Artificial Neural Network (ANN) to predict the viscosity of Silver/Ethylene glycol nanofluid at different temperatures and volume fraction of nanoparticles. *Physica A* 2019;534:122142.
- [123] Mohamadian F, Eftekhar L, Haghghi Bardineh Y. Applying GMDH artificial neural network to predict dynamic viscosity of an antimicrobial nanofluid. *Nanomed J* 2018;5(4):217–21.
- [124] Esfe MH, et al. Evaluation of thermal conductivity of COOH-functionalized MWCNTs/water via temperature and solid volume fraction by using experimental data and ANN methods. *J Therm Anal Calorim* 2015;121(3):1273–8.
- [125] Esfe MH, et al. Using artificial neural network to predict thermal conductivity of ethylene glycol with alumina nanoparticle. *J Therm Anal Calorim* 2016;126(2):643–8.
- [126] Hemmati-Sarapardeh A, et al. On the evaluation of the viscosity of nanofluid systems: modeling and data assessment. *Renew Sustain Energy Rev* 2018;81:313–29.
- [127] Toghyani S, et al. Artificial neural network, ANN-PSO and ANN-ICA for modelling the Stirling engine. *Int J Ambient Energy* 2016;37(5):456–68.
- [128] Loni R, et al. ANN model to predict the performance of parabolic dish collector with tubular cavity receiver. *Mech Ind* 2017;18(4):408.
- [129] Ahmadi MH, et al. Application GMDH artificial neural network for modeling of Al₂O₃/water and Al₂O₃/ethylene glycol thermal conductivity. *Int J Heat Technol* 2018;36(3):773–82.
- [130] Vickers NJ. Animal communication: when i'm calling you, will you answer too? *Curr Biol* 2017;27(14):R713–5.
- [131] Aberoumand S, et al. Experimental study on the rheological behavior of silver–heat transfer oil nanofluid and suggesting two empirical based correlations for thermal conductivity and viscosity of oil based nanofluids. *Appl Therm Eng* 2016;101:362–72.
- [132] Esfe MH, et al. Rheological characteristics of MgO/oil nanolubricants: experimental study and neural network modeling. *Int Commun Heat Mass Transf* 2017;86:245–52.
- [133] Afrand M, et al. Predicting the viscosity of multi-walled carbon nanotubes/water nanofluid by developing an optimal artificial neural network based on experimental data. *Int Commun Heat Mass Transf* 2016;77:49–53.
- [134] Esfe MH, et al. Designing an artificial neural network to predict dynamic viscosity of aqueous nanofluid of TiO₂ using experimental data. *Int Commun Heat Mass Transf* 2016;75:192–6.
- [135] Rezaei MH, et al. Applying GMDH artificial neural network in modeling CO₂ emissions in four nordic countries. *Int J Low Carbon Technol* 2018;13(3):266–71.
- [136] Shahsavari A, et al. A novel comprehensive experimental study concerned synthesizes and prepare liquid paraffin-Fe3O₄ mixture to develop models for both thermal conductivity & viscosity: a new approach of GMDH type of neural network. *Int J Heat Mass Transf* 2019;131:432–41.
- [137] Mei X, et al. Development of the ANN-KIM composed model to predict the nanofluid energetic thermal conductivity via various types of nano-powders dispersed in oil. *J Therm Anal Calorim* 2020;1–6.
- [138] Esfe MH, et al. An experimental study on the effect of diameter on thermal conductivity and dynamic viscosity of Fe/water nanofluids. *J Therm Anal Calorim* 2015;119(3):1817–24.
- [139] Esfe MH, et al. Designing an artificial neural network to predict thermal conductivity and dynamic viscosity of ferromagnetic nanofluid. *Int Commun Heat Mass Transf* 2015;68:50–7.
- [140] Žmak I, Filetin T. Predicting thermal conductivity of steels using artificial neural networks. *Trans FAMENA* 2010;34(3).
- [141] Atashrouz S, Pazuki G, Alimoradi Y. Estimation of the viscosity of nine nanofluids using a hybrid GMDH-type neural network system. *Fluid Phase Equilib* 2014;372:43–8.

- [142] Aminian A. Predicting the effective viscosity of nanofluids for the augmentation of heat transfer in the process industries. *J Mol Liq* 2017;229:300–8.
- [143] Kumar DD, Arasu AV. A comprehensive review of preparation, characterization, properties and stability of hybrid nanofluids. *Renew Sustain Energy Rev* 2018;81:1669–89.
- [144] Esfe MH, et al. Estimation of thermal conductivity of ethylene glycol-based nanofluid with hybrid suspensions of SWCNT-Al₂O₃ nanoparticles by correlation and ANN methods using experimental data. *J Therm Anal Calorim* 2017;128(3):1359–71.
- [145] Maddah H, et al. Factorial experimental design for the thermal performance of a double pipe heat exchanger using Al₂O₃-TiO₂ hybrid nanofluid. *Int Commun Heat Mass Transf* 2018;97:92–102.
- [146] Esfe MH, et al. Experimental determination of thermal conductivity and dynamic viscosity of Ag-MgO/water hybrid nanofluid. *Int Commun Heat Mass Transf* 2015;66:189–95.
- [147] Asadi A, et al. The effect of temperature and solid concentration on dynamic viscosity of MWCNT/MgO (20–80)–SAE50 hybrid nano-lubricant and proposing a new correlation: an experimental study. *Int Commun Heat Mass Transf* 2016;78:48–53.
- [148] Maddah H, et al. Prediction and modeling of MWCNT/Carbon (60/40)/SAE 10W 40/SAE 85W 90 (50/50) nanofluid viscosity using artificial neural network (ANN) and self-organizing map (SOM). *J Therm Anal Calorim* 2018;134(3):2275–86.
- [149] Esfe MH, et al. Modeling and prediction of rheological behavior of Al₂O₃-MWCNT/SW50 hybrid nano-lubricant by artificial neural network using experimental data. *Physica A* 2018;510:625–34.
- [150] Akhgar A, et al. Developing dissimilar artificial neural networks (ANNs) to prediction the thermal conductivity of MWCNT-TiO₂/Water-ethylene glycol hybrid nanofluid. *Powder Technol* 2019;355:602–10.
- [151] Hassanpour M, Vaferi B, Masoumi ME. Estimation of pool boiling heat transfer coefficient of alumina water-based nanofluids by various artificial intelligence (AI) approaches. *Appl Therm Eng* 2018;128:1208–22.
- [152] Hojjat M, et al. Thermal conductivity of non-Newtonian nanofluids: experimental data and modeling using neural network. *Int J Heat Mass Transf* 2011;54(5–6):1017–23.
- [153] Hassan MA, Banerjee D. A soft computing approach for estimating the specific heat capacity of molten salt-based nanofluids. *J Mol Liq* 2019;281:365–75.
- [154] Kalani H, Sardarabadi M, Passandideh-Fard M. Using artificial neural network models and particle swarm optimization for manner prediction of a photovoltaic thermal nanofluid based collector. *Appl Therm Eng* 2017;113:1170–7.
- [155] Baghban A, et al. Sensitivity analysis and application of machine learning methods to predict the heat transfer performance of CNT/water nanofluid flows through coils. *Int J Heat Mass Transf* 2019;128:825–35.
- [156] Alrashed AA, et al. Effects on thermophysical properties of carbon based nanofluids: experimental data, modelling using regression, ANFIS and ANN. *Int J Heat Mass Transf* 2018;125:920–32.
- [157] Wang Q, et al. Prediction of heat transfer rates for shell-and-tube heat exchangers by artificial neural networks approach. *J Therm Sci* 2006;15(3):257–62.
- [158] Xie G, et al. Heat transfer analysis for shell-and-tube heat exchangers with experimental data by artificial neural networks approach. *Appl Therm Eng* 2007;27(5–6):1096–104.
- [159] Xie G, et al. Performance predictions of laminar and turbulent heat transfer and fluid flow of heat exchangers having large tube-diameter and large tube-row by artificial neural networks. *Int J Heat Mass Transf* 2009;52(11–12):2484–97.
- [160] Zdaniuk GJ, Chamra LM, Walters DK. Correlating heat transfer and friction in helically-finned tubes using artificial neural networks. *Int J Heat Mass Transf* 2007;50(23–24):4713–23.
- [161] Zdaniuk GJ, et al. A comparison of artificial neural networks and symbolic-regression-based correlations for optimization of helically finned tubes in heat exchangers. *J Enhanced Heat Transf* 2011;18(2).
- [162] Bokde N, et al. A review on hybrid empirical mode decomposition models for wind speed and wind power prediction. *Energies* 2019;12(2):254.
- [163] Maddah H, et al. Experimental and numerical study of nanofluid in heat exchanger fitted by modified twisted tape: exergy analysis and ANN prediction model. *Heat Mass Transf* 2017;53(4):1413–23.
- [164] Nasirzadehroshenin F, Maddah H, Sakhaeinia H. Investigation of exergy of double-pipe Heat exchanger using synthesized hybrid nanofluid developed by modeling. *Int J Thermophys* 2019;40(9):87.
- [165] Nasirzadehroshenin F, Maddah H, Sakhaeinia H. Investigation of exergy of double-pipe heat exchanger using synthesized hybrid nanofluid developed by modeling. *Int J Thermophys* 2019;40(9):1–24.
- [166] Safikhani H, et al. Multi-objective optimization of nanofluid flow in flat tubes using CFD, Artificial Neural Networks and genetic algorithms. *Adv Powder Technol* 2014;25(5):1608–17.
- [167] Bahiraei M, Khosravi R, Heshmatian S. Assessment and optimization of hydrothermal characteristics for a non-Newtonian nanofluid flow within miniaturized concentric-tube heat exchanger considering designer's viewpoint. *Appl Therm Eng* 2017;123:266–76.
- [168] Hojjat M. Nanofluids as coolant in a shell and tube heat exchanger: ANN modeling and multi-objective optimization. *Appl Math Comput* 2020;365:124710.
- [169] Elsheikh AH, et al. Modeling of solar energy systems using artificial neural network: a comprehensive review. *Sol Energy* 2019;180:622–39.
- [170] Rashidi S, Karimi N, Yan WM. Applications of machine learning techniques in performance evaluation of solar desalination systems–A concise review. *Eng Anal Bound Elem* 2022;144:399–408.
- [171] De Risi A, Milanese M, Laforgia D. Modelling and optimization of transparent parabolic trough collector based on gas-phase nanofluids. *Renew Energy* 2013;58:134–9.
- [172] Toghiani S, Baniasadi E, Afshari E. Thermodynamic analysis and optimization of an integrated Rankine power cycle and nano-fluid based parabolic trough solar collector. *Energy Convers Manage* 2016;121:93–104.
- [173] Boyaghchi FA, Mahmoodnezhad M, Sabeti V. Exergoeconomic analysis and optimization of a solar driven dual-evaporator vapor compression-absorption cascade refrigeration system using water/CuO nanofluid. *J Clean Prod* 2016;139:970–85.
- [174] Tomy AM, et al. Analysing the performance of a flat plate solar collector with silver/water nanofluid using artificial neural network. *Procedia Comput Sci* 2016;93:33–40.
- [175] Sadeghi G, et al. Energy and exergy evaluation of the evacuated tube solar collector using Cu₂O/water nanofluid utilizing ANN methods. *Sustain Energy Technol Assess* 2020;37:10057.
- [176] Ajbar W, et al. The multivariable inverse artificial neural network combined with GA and PSO to improve the performance of solar parabolic trough collector. *Appl Therm Eng* 2021;189:116651.
- [177] Yousef JH, et al. A comparison study based on artificial neural network for assessing PV/T solar energy production. *Case Stud Therm Eng* 2019;13:100407.
- [178] Selimefendigil F, Öztop HF, Afrand M. Shape effects of TEG mounted ventilated cavities with alumina-water nanofluids on the performance features by using artificial neural networks. *Eng Anal Bound Elem* 2022;140:79–97.
- [179] Liu H, et al. Optimization study of thermal-storage PV-CSP integrated system based on GA-PSO algorithm. *Sol Energy* 2019;184:391–409.
- [180] Esmaili Z, et al. Effects of hybrid nanofluids and turbulator on efficiency improvement of parabolic trough solar collectors. *Eng Anal Bound Elem* 2023;148:1114–25.
- [181] Shabbak MH. Advances in solar photovoltaics: technology review and patent trends. *Renew Sustain Energy Rev* 2019;115:109383.
- [182] Mertens K. Photovoltaics: fundamentals, technology, and practice. John Wiley & Sons; 2018.
- [183] Ebrahimi-Moghadam A, Mohseni-Gharyehsafa B, Farzaneh-Gord M. Using artificial neural network and quadratic algorithm for minimizing entropy generation of Al₂O₃-EG/W nanofluid flow inside parabolic trough solar collector. *Renew Energy* 2018;129:473–85.
- [184] Delfani S, Esmaili M, Karami M. Application of artificial neural network for performance prediction of a nanofluid-based direct absorption solar collector. *Sustain Energy Technol Assess* 2019;36:100559.
- [185] Al-Waeli AH, et al. Artificial neural network modeling and analysis of photovoltaic/thermal system based on the experimental study. *Energy Convers Manage* 2019;186:368–79.
- [186] Al-Waeli AH, et al. Comparison of prediction methods of PV/T nanofluid and nano-PCM system using a measured dataset and artificial neural network. *Sol Energy* 2018;162:378–96.
- [187] Li X, Wang CH. 2017 PV Danckwerts Memorial Lecture special issue editorial: advances in emerging technologies of chemical engineering towards sustainable energy and environment: solar and biomass. *Chem Eng Sci* 2020;215:115384.
- [188] Kim C, et al. A hybrid organic-inorganic perovskite dataset. *Sci Data* 2017;4(1):1–11.
- [189] Schmidt J, et al. Predicting the thermodynamic stability of solids combining density functional theory and machine learning. *Chem Mater* 2017;29(12):5090–103.
- [190] Allam O, et al. Density functional theory-machine learning approach to analyze the bandgap of elemental halide perovskites and ruddlesden-popper phases. *ChemPhysChem* 2018;19(19):2559–65.
- [191] Lu S, et al. Accelerated discovery of stable lead-free hybrid organic-inorganic perovskites via machine learning. *Nat Commun* 2018;9(1):1–8.
- [192] Takahashi K, et al. Searching for hidden perovskite materials for photovoltaic systems by combining data science and first principle calculations. *ACS Photonics* 2018;5(3):771–5.
- [193] Xu Q, et al. Rationalizing perovskite data for machine learning and materials design. *J Phys Chem Lett* 2018;9(24):6948–54.
- [194] Choudhary K, et al. Accelerated discovery of efficient solar cell materials using quantum and machine-learning methods. *Chem Mater* 2019;31(15):5900–8.
- [195] Im J, et al. Identifying Pb-free perovskites for solar cells by machine learning. *njp Comput Mater* 2019;5(1):1–8.
- [196] Jain D, et al. Bulk and surface DFT investigations of inorganic halide perovskites screened using machine learning and materials property databases. *Phys Chem Chem Phys* 2019;21(35):19423–36.
- [197] Li C, et al. Formability of ABX₃ (X = F, Cl, Br, I) Halide Perovskites. *Acta Crystallogr, Sect B: Struct Sci* 2008;64(6):702–7.
- [198] Pilania G, et al. Finding new perovskite halides via machine learning. *Front Mater* 2016;3:19.
- [199] Ma XY, et al. Accelerated discovery of two-dimensional optoelectronic octahedral oxyhalides via high-throughput ab initio calculations and machine learning. *J Phys Chem Lett* 2019;10(21):6734–40.
- [200] Li J, et al. Predictions and strategies learned from machine learning to develop high-performing perovskite solar cells. *Adv Energy Mater* 2019;9(46):1901891.
- [201] Odabaşı Ç, Yıldırım R. Performance analysis of perovskite solar cells in 2013–2018 using machine-learning tools. *Nano Energy* 2019;56:770–91.
- [202] Oviedo F, et al. Fast and interpretable classification of small X-ray diffraction datasets using data augmentation and deep neural networks. *njp Comput Mater* 2019;5(1):1–9.

- [203] Hartono NTP, et al. How machine learning can help select capping layers to suppress perovskite degradation. *Nat Commun* 2020;11(1):1–9.
- [204] Odabaşı Ç, Yıldırım R. Assessment of reproducibility, hysteresis, and stability relations in perovskite solar cells using machine learning. *Energy Technol* 2020;8(12):1901449.
- [205] Raza MQ, Nadarajah M, Ekanayake C. On recent advances in PV output power forecast. *Sol Energy* 2016;136:125–44.
- [206] Diagne M, et al. Review of solar irradiance forecasting methods and a proposition for small-scale insular grids. *Renew Sustain Energy Rev* 2013;27:65–76.
- [207] Voyant C, et al. Machine learning methods for solar radiation forecasting: a review. *Renew Energy* 2017;105:569–82.
- [208] Shivashankar S, et al. Mitigating methods of power fluctuation of photovoltaic (PV) sources—A review. *Renew Sustain Energy Rev* 2016;59:1170–84.
- [209] Raza MQ, Khosravi A. A review on artificial intelligence based load demand forecasting techniques for smart grid and buildings. *Renew Sustain Energy Rev* 2015;50:1352–72.
- [210] de Marcos RA, Bello A, Reneses J. Electricity price forecasting in the short term hybridising fundamental and econometric modelling. *Electric Power Syst Res* 2019;167:240–51.
- [211] Ren Y, Suganthan P, Srikanth N. Ensemble methods for wind and solar power forecasting—A state-of-the-art review. *Renew Sustain Energy Rev* 2015;50:82–91.
- [212] Das UK, et al. Forecasting of photovoltaic power generation and model optimization: a review. *Renew Sustain Energy Rev* 2018;81:912–28.
- [213] Behera MK, Majumder I, Nayak N. Solar photovoltaic power forecasting using optimized modified extreme learning machine technique. *Eng Sci Technol Int J* 2018;21(3):428–38.
- [214] Zhang J, et al. Deep photovoltaic nowcasting. *Sol Energy* 2018;176:267–76.
- [215] Almonacid F, et al. A methodology based on dynamic artificial neural network for short-term forecasting of the power output of a PV generator. *Energy Convers Manage* 2014;85:389–98.
- [216] Zhang J, et al. A suite of metrics for assessing the performance of solar power forecasting. *Sol Energy* 2015;111:157–75.
- [217] Shi J, et al. Forecasting power output of photovoltaic systems based on weather classification and support vector machines. *IEEE Trans Ind Appl* 2012;48(3):1064–9.
- [218] Wang F, et al. Solar irradiance feature extraction and support vector machines based weather status pattern recognition model for short-term photovoltaic power forecasting. *Energy Build* 2015;86:427–38.
- [219] Wang F, et al. Comparative study on KNN and SVM based weather classification models for day ahead short term solar PV power forecasting. *Appl Sci* 2018;8(1):28.
- [220] Stehman SV. Selecting and interpreting measures of thematic classification accuracy. *Remote Sens Environ* 1997;62(1):77–89.
- [221] Das UK, et al. SVR-based model to forecast PV power generation under different weather conditions. *Energies* 2017;10(7):876.
- [222] Lima FJ, et al. Forecast for surface solar irradiance at the Brazilian Northeastern region using NWP model and artificial neural networks. *Renew Energy* 2016;87:807–18.
- [223] Kasten F, Czeplak G. Solar and terrestrial radiation dependent on the amount and type of cloud. *Sol Energy* 1980;24(2):177–89.
- [224] Nann S, Riordan C. Solar spectral irradiance under clear and cloudy skies: measurements and a semiempirical model. *J Appl Meteorol Climatol* 1991;30(4):447–62.
- [225] Kaskaoutis D, et al. Modification of solar radiation components under different atmospheric conditions in the Greater Athens Area, Greece. *J Atmos Sol Terr Phys* 2006;68(10):1043–52.
- [226] Sun Y, et al. Correlation feature selection and mutual information theory based quantitative research on meteorological impact factors of module temperature for solar photovoltaic systems. *Energies* 2017;10(1):7.
- [227] Al-Dahidi S, et al. Ensemble approach of optimized artificial neural networks for solar photovoltaic power prediction. *IEEE Access* 2019;7:81741–58.
- [228] Bui KTT, et al. A novel hybrid artificial intelligent approach based on neural fuzzy inference model and particle swarm optimization for horizontal displacement modeling of hydropower dam. *Neural Comput Appl* 2018;29(12):1495–506.
- [229] Bui DT, et al. Hybrid intelligent model based on least squares support vector regression and artificial bee colony optimization for time-series modeling and forecasting horizontal displacement of hydropower dam. *Handbook of neural computation*. Elsevier; 2017. p. 279–93.
- [230] Hegazy T, Fazio P, Moselhi O. Developing practical neural network applications using back-propagation. *Comput Aided Civ Infrastruct Eng* 1994;9(2):145–59.
- [231] Bui DT, Nhu VH, Hoang ND. Prediction of soil compression coefficient for urban housing project using novel integration machine learning approach of swarm intelligence and multi-layer perceptron neural network. *Adv Eng Inf* 2018;38:593–604.
- [232] Elman J. Finding structure in time. *Cogn Sci* 1990;14(2):179–212.
- [233] Williams RJ, Zipser D. Experimental analysis of the real-time recurrent learning algorithm. *Conn Sci* 1989;1(1):87–111.
- [234] Al-Dahidi S, et al. Extreme learning machines for solar photovoltaic power predictions. *Energy* 2018;11(10):2725.
- [235] Paulescu M, et al. Structured, physically inspired (gray box) models versus black box modeling for forecasting the output power of photovoltaic plants. *Energy* 2017;121:792–802.
- [236] Wang X, Yang K, Kalivas JH. Comparison of extreme learning machine models for gasoline octane number forecasting by near-infrared spectra analysis. *Optik* 2020;200:163325 (Stuttg).
- [237] Hossain M, et al. Application of extreme learning machine for short term output power forecasting of three grid-connected PV systems. *J Clean Prod* 2017;167:395–405.
- [238] Pelland S, et al. Photovoltaic and solar forecasting: state of the art. IEA PVPS, Task 2013;14(2013):1–36.
- [239] Sharma V, et al. Short term solar irradiance forecasting using a mixed wavelet neural network. *Renew Energy* 2016;90:481–92.
- [240] Pedro HT, Coimbra CF. Short-term irradiance forecastability for various solar micro-climates. *Sol Energy* 2015;122:587–602.
- [241] Ramsami P, Oree V. A hybrid method for forecasting the energy output of photovoltaic systems. *Energy Convers Manage* 2015;95:406–13.
- [242] Liu J, et al. An improved photovoltaic power forecasting model with the assistance of aerosol index data. *IEEE Trans Sustain Energy* 2015;6(2):434–42.
- [243] Lu H, Chang G. A hybrid approach for day-ahead forecast of PV power generation. *IFAC-PapersOnLine* 2018;51(28):634–8.
- [244] Izgi E, et al. Short-mid-term solar power prediction by using artificial neural networks. *Sol Energy* 2012;86(2):725–33.
- [245] Dahmani K, et al. Estimation of 5-min time-step data of tilted solar global irradiation using ANN (Artificial Neural Network) model. *Energy* 2014;70:374–81.
- [246] Paoli C, et al. Forecasting of preprocessed daily solar radiation time series using neural networks. *Sol Energy* 2010;84(12):2146–60.
- [247] Sivaneesan B, Yu C, Goh K. Solar forecasting using ANN with fuzzy logic pre-processing. *Energy Procedia* 2017;143:727–32.
- [248] Chu Y, et al. Short-term reforecasting of power output from a 48 MWe solar PV plant. *Sol Energy* 2015;112:68–77.
- [249] Jamali B, et al. Using PSO-GA algorithm for training artificial neural network to forecast solar space heating system parameters. *Appl Therm Eng* 2019;147:647–60.
- [250] Huang Y, et al. Comparative study of power forecasting methods for PV stations. In: Proceedings of the 2010 international conference on power system technology. IEEE; 2010.